
Article:
Sultan, A.J. orcid.org/0000-0002-1635-0342, Ingham, D.B. orcid.org/0000-0002-4633-0852, Ma, L. orcid.org/0000-0002-3731-8464 et al. (2 more authors) (2023) Comparative techno-economic assessment and minimization of the levelized cost of electricity for increasing capacity wind power plants by row and angle layout optimization. Journal of Cleaner Production, 430. 139578. ISSN: 0959-6526

https://doi.org/10.1016/j.jclepro.2023.139578

Journal of Cleaner Production 430 (2023) 139578

Contents lists available at ScienceDirect

Journal of Cleaner Production

journal homepage: www.elsevier.com/locate/jclepro

Comparative techno-economic assessment and minimization of the levelized cost of electricity for increasing capacity wind power plants by row and angle layout optimization

Ali J. Sultan [a], Derek B. Ingham [b], Lin Ma [b], Kevin J. Hughes [b,*], Mohamed Pourkashanian [b]

[a] Energy and Building Research Center, Kuwait Institute for Scientific Research, Al-Jaheth Street, Shuwaikh Educational Area, P.O. Box 24885, Safat, 13109, Kuwait
[b] Energy 2050, Department of Mechanical Engineering, University of Sheffield, Sheffield, S3 7RD, United Kingdom

ARTICLE INFO

Handling editor: Jin-Kuk Kim

Keywords:
Wind power
Optimization
Performance assessment
LCOE
Optimal layout angle
Kuwait

ABSTRACT

This work presents techno-economic assessment and optimization results for wind power implementation. The results constitute an attempt to provide recommendations on optimal design configurations and operating conditions for future possibilities of installations in Kuwait, where the wind speed is at maximum levels at high altitudes during the early daytime and late nighttime, whereas in the afternoon, the wind speed reaches its maximum at low altitudes. This cyclic behavior indicates that the wind speed and direction change in a predictable pattern, benefiting wind power generation. The techno-economic assessment and optimization are performed for multi-row design configurations of power plants. The selection using an optimal method comes through evaluating 2220 configurations, from which 60 optimal configurations are determined for different variations of the number of rows in the wind power plant (N_r) based on the minimization criterion of the Levelized Cost of Electricity (LCOE). The optimal configurations have optimal wind power plant layout angle (θ_{plant}). Some of the main findings are as follows:(i) the N_r and θ_{plant} values impact the LCOE, wake losses, performance ratio, capacity factor, and annual gross energy. (ii) The wind power density is calculated to be 289 W/m^2, (iii) June and July have high levels of generation, wind speed, temperature, and humidity, (iv) there exists an exponential relation between the installed cost per watt and N_r. (v) The present value of annual energy, net present value (annual costs), annual energy, and annual gross energy have increasing linear trends as N_r increases, and (vi) the optimal configurations require a power purchase agreement price of at least 7.03 cent/kWh to make a positive return on investment.

1. Introduction

The main goal of this study is to assess the economic and technological factors associated with wind power plants used for generating electricity in arid climates. Furthermore, the goal is to facilitate the adoption of renewable technology in the Middle East and North Africa (MENA) region, including the Gulf Cooperation Council (GCC), to realize large-scale power plans as highlighted in previous research (Sultan et al., 2020a, 2020b, Sultan, 2021a, 2021b). Fig. S. 1 provides a visual representation of the locations of select countries in the MENA/GCC region, along with a detailed map of Kuwait, the selected location in this work. There are several justifications for investigating the Kuwait case. There is a scarcity of published literature that provides a comprehensive evaluation of the techno-economics of wind power technology specifically tailored to the prevailing conditions in Kuwait, which is characterized by an arid climate. The investigated location is known to experience extreme weather conditions. For instance, in July 2016, the maximum temperature reached 54 °C (129.2 °F) in the shade, reported as one of the highest reliably measured air temperatures ever recorded on Earth. These extreme conditions make Kuwait an exciting and unique case for studying the performance and feasibility of wind power technology (Fletcher, 2016; Burt, 2016a, 2016b; Livingston, 2019; WMO, 2019). Further, Kuwait has heavily subsidized electricity prices, particularly from fossil-based plants, with a rate of 0.66 cent/kWh, as shown in Table S. 1 and Table S. 2 (IRENA, 2016, 2014; Hertog, 2013). Hence, the case of Kuwait presents a promising opportunity to assess the techno-economic competitiveness of green energy, specifically wind power. Given its heavily subsidized prices of fossil-based electricity, evaluating wind power's feasibility and

* Corresponding author.
E-mail address: k.j.hughes@sheffield.ac.uk (K.J. Hughes).

https://doi.org/10.1016/j.jclepro.2023.139578
Received 26 July 2023; Received in revised form 20 September 2023; Accepted 30 October 2023
Available online 6 November 2023

Nomenclature: Acronyms

AFPs	Annual Frequency Profile(s)
CSP-PT	Concentrating Solar Power - Parabolic Trough
CAPEX	Capital expenses
GCC	Gulf Cooperation Council
GHG	Greenhouse Gas
HFPs	Hourly Frequency Profile(s)
LOESS	Locally Estimated Scatterplot Smoothing (regression)
MENA	Middle East and North Africa
MFPs	Monthly Frequency Profile(s)
OPEX	Operating expenses
PPA	Power Purchase Agreement
RLCs	Reference Level of Calculation(s) (RLCs)
SAM	System Advisor Model
TES	Thermal Energy Storage
TRNSYS	Transient System Simulation

Units

bbl	barrel of oil
MW_h	Megawatt hour
MW_e	Megawatt electric
MWh_e	Megawatt hour electric
MWh_t	Megawatt hour thermal

Symbols

A_b	Wind turbine blade area/blade's swept area (m^2)
AEP	Annual Electricity Production (kWh)
C_p	Wind turbine power coefficient (%)
FCR	Fixed Charge Rate (−)
FOC	Fixed annual operating cost or operations and maintenance costs ($)
TCC	Installed Capital Cost ($)
LCOE	Levelized Cost of Electricity (cent/kWh)
n	Time period (−)
N_r	Number of rows in the wind power plant (−)
P_w	The output of the wind power-generating unit (kW)
u_h	Wind speed at the wind turbine's hub height (m/s)
u_1	Wind speed at a higher altitude (m/s)
u_2	Wind speed at a lower altitude (m/s)
VOC	Variable operating cost or operations and maintenance costs per unit of annual electricity production ($/kWh)
z_1	Higher altitude (m)
z_2	Lower altitude (m)

Greek Symbols

α	Wind shear/exponent (−)
θ_{plant}	Wind power plant layout angle (°)
ρ	Air density (kg/ m^3)

economic viability in this context becomes even more significant. This assessment will provide valuable insights into the potential of wind power to compete and contribute to the energy transition in Kuwait.

Additionally, Kuwait has set a strategic target of achieving a 15% penetration of renewable energy in its electricity demand by 2030. However, the specific technology mix to achieve this target has not been entirely determined yet. This highlights the importance of conducting assessments and studies, such as this one, to evaluate wind power's potential contributions toward meeting Kuwait's renewable energy goals. By exploring various options and conducting a detailed techno-economic analysis, the study can provide valuable insights for policy-makers in determining the optimal technology mix to achieve the country's renewable energy target commitment.

Furthermore, Kuwait is a member of the MENA/GCC and part of a regional alliance that promotes cooperation and collaboration in various areas, including energy. This allows Kuwait to engage in regional discussions, share best practices, and align its renewable energy efforts with broader goals and initiatives. This membership further emphasizes the significance of investigating wind power, as it contributes to the regional efforts towards sustainable and clean energy development.

On top of that, the government's exclusive ownership of the electricity sector in Kuwait, coupled with its heavy reliance on fossil fuels, underlines the importance of assessing the performance of wind power for electricity generation. By exploring wind power feasibility and potential, this study can contribute to diversifying the country's energy mix, reducing its dependence on fossil fuels, and promoting oil conservation efforts. Introducing wind power can help move towards a more sustainable and environmentally friendly energy system while reducing carbon footprint and contributing to global efforts in combating climate change.

In 2005, Kuwait had held one of the world's lowest comparative prices of residential electricity. This indicates that electricity was relatively affordable for residential consumers compared to other countries. However, it is essential to note that electricity prices can change over time and vary based on multiple factors, such as energy sources, subsidies, and market conditions. Assessing and implementing wind power can contribute to maintaining affordable electricity prices while promoting sustainable and environmentally friendly energy solutions (Atalla and Hunt, 2016).

In 2010, Kuwait had held one of the world's largest comparative size of per capita residential electricity consumption. This indicates that, on average, the residents consumed a significant amount of electricity compared to residents of other countries during that time. High per capita electricity consumption can be attributed to a high standard of living, energy-intensive industries, and a reliance on air conditioning due to the extreme climate. However, it is essential to promote energy efficiency measures and wind power to reduce the environmental impact and ensure sustainable energy consumption patterns in the long term (Atalla and Hunt, 2016).

Additionally, when examining electricity usage and carbon dioxide (CO_2) emissions, Kuwait is positioned among the leading nations., as depicted in Fig. S. 2 (Atalla and Hunt, 2016; World Bank, 2019b; Ritchie and Roser, 2014, 2017; Khatti and Woodruff, 2021). Kuwait is renowned for its exceptionally subsidized electricity prices, one of the lowest rates globally at 0.66 cent/kWh produced by fossil-fuel power plants, as shown in Fig. S. 3 (see Table S. 1 and Table S. 2) (IRENA, 2016, 2014; Hertog, 2013). It is important to note that the Levelized Cost of Electricity (LCOE) related to wind power technology has become increasingly competitive and now falls within the range of global fossil-fuel costs. Moreover, further reductions in LCOE for wind power are anticipated in the coming years (see Fig. S. 4) since the capacity of a wind power plant has a notable impact on the LCOE due to its economy of scale.

This study focuses on a location (Shagaya, Kuwait) with minimal concentrations of oil and gas fields and is characterized by abundant wind resources with high potential (Shams et al., 2017; Alhajraf and Heil, 2011). Upon analyzing the configuration of Kuwait's transmission networks, taking into account their layout and structure (GENI, 2017), the analysis reveals that the selected location has the potential to maximize its future network capacity factor. This can be achieved by strategically allocating shares of renewable power technology based on the overlapping peaks in solar and wind resources. Considering this approach, minimizing the LCOE through hybridizing renewable technologies is possible. Solar power technologies like the Concentrating Solar Power - Parabolic Trough (CSP-PT) technology with Thermal Energy Storage (TES) offer dispatchability, making it even more

advantageous for reducing LCOE through renewable technology hybridization (ISES, 2018). It is worth noting that wind power usually is not dispatchable, unlike solar power. However, other grid services, such as spinning reserves, can be utilized, providing the option to incorporate dispatchable power sources. Fig. S. 5 shows that the chosen location in the western region has minimal oil and gas field concentrations. Additionally, Fig. S .6 depicts a map of Kuwait, highlighting the western region with limited transmission networks. It is crucial to recognize that this location's future network capacity factor can be maximized due to the significant solar and wind resources. Consequently, conducting a detailed assessment and optimization to minimize the LCOE for wind power plants is highly recommended, underlining the importance of this work.

As previously stated, the selected location benefits from abundant solar and wind resources at their peak levels. Additionally, this location has minimal concentrations of oil and gas fields (Mirza, 2018; Alhajraf and Heil, 2011; Alnassar et al., 2005; SolarGIS, 2019; Shams et al., 2017). Hence, harnessing wind power technology for electricity generation can offer significant economic benefits for Kuwait when compared to the current business-as-usual approach of relying on conventional fossil-based power plants and selling electricity at heavily subsidized rates as low as 0.66 cent/kWh (see Table S. 1 and Table S. 2). Generally, most electricity consumers in Kuwait belong to the residential sector and benefit from significant subsidies, paying only around 6% of the actual average cost of electricity. It is essential to highlight that the average actual cost of electricity in conventional power plants in Kuwait is 14 cent/kWh (Ali and Alsabbagh, 2018; Ansari, 2013; Alrai, 2015).

Kuwait possesses approximately 102 Gbbl of oil reserves, which accounts for around 6% of the global reserve, placing it in the sixth position. Furthermore, the oil sector contributes 40% to the country's gross domestic product and 92% to its export revenues. Nevertheless, relying heavily on oil exports is no longer sustainable due to unpredictable market shifts worldwide. As a result, Kuwait has initiated preliminary research on natural resources and assessments of renewable energy technologies, which have acted as driving factors in considering the implementation of significant renewable energy projects in the future (Alhajraf et al., 2011; Alhajraf and Heil, 2011; Alnassar et al., 2005; Al-Rasheedi et al., 2015; Sultan and Alotaibi, 2016; Sultan, 2017; Sebzali et al., 2016). The studies share a unified objective: protecting Kuwait's natural resources and preserving the environment (Alrashidi et al., 2011). Kuwait has a total land area of approximately 17,818 km^2 (A Al-Dousari et al., 2018), mainly of flat desert terrain. While research on wind power in Kuwait is limited, none of the published studies has provided a comprehensive performance assessment and optimization of wind power, explicitly considering Kuwait's unique climatic conditions. This indicates the need for a detailed investigation and analysis to evaluate the feasibility, optimization, and potential of wind power generation in Kuwait, as attempted in this work. For further details, refer to Appendix A, Appendix B, figures from Fig. S. 7 to Fig. S. 30 (Appendix F), and Table S .3 to Table S. 8 for background information and supplementary data about Kuwait, MENA, and GCC region.

1.1. Aim and technology selection

In a typical wind power plant, the most effective method to increase the energy yield is to accurately predict wind availability, directly impacting electricity generation from wind turbines. Extending this understanding to the entire plant's lifetime emphasizes the importance of a reliable and detailed wind resource assessment before the design and optimization stages to maximize wind availability estimation for a specific location. In addition to reliable resource assessment at the wind turbine's hub height, understanding the turbine design characteristics, such as the power curve, is critical for predicting energy generation accurately. Based on physical principles, the prevailing wind's kinetic energy is the primary determinant that allows wind energy extraction through the turbines' blades when sufficient wind speeds are encountered. Generally, wind density is influenced significantly by ambient temperature, atmospheric pressure, and relative humidity. Thus, wind density and speed define the kinetic energy in the blowing wind (see Appendix D). However, the ambient temperature is extremely high in a desert region like Kuwait. Hence, the impact of harsh conditions should be investigated, along with the wind resource and wind turbine's design characteristics, significantly since the wind resource can be affected by complex factors impacting the reliability and feasibility of generation.

Wind speed and direction measurements should be obtained at the reference wind turbine's hub height. Furthermore, estimating the wind shear (α), which is the change in the wind speed with height above ground, is critical. The value of α indicates the variation or difference in wind speed and direction over a vertical distance. Knowing an accurate value of α promotes the efficient conversion of wind energy into electricity, making wind power generation more predictable. By harnessing reliable wind resources, wind power projects can take advantage of wind patterns and contribute to generating clean and renewable energy. In addition, ambient temperature, atmospheric pressure, and relative humidity are necessary for density calculation, as they directly affect the turbine's power output.

The primary aim of this study is to conduct a techno-economic evaluation and optimize the design configurations of wind power plants for electricity generation that are well-suited to the Kuwait desert's wind and climatic conditions. It should be recalled that the chosen location is approximately 100 km from the capital city. Additionally, it is at an elevation of roughly 240 m above sea level. Furthermore, it is characterized by a plain topography and simple terrain without significant obstacles from the surroundings that would influence the wind and disturb its flow. Also, it has no existing vegetation and obstructions that would promote shading effects or wind disturbances. Another main objective is to perform detailed parametric analyses and identify optimal design configurations for wind power plants with various capacity ratings. The chosen location has an existing 10 MW wind power plant (5 × 2 MW), the first wind power plant in Kuwait with a recent commission date. After one year of operation, it was revealed that the plant had produced energy production numbers that exceeded the industry average (A Al-Dousari et al., 2019; Ali and Alsabbagh, 2018; Al-Nassar et al., 2019; Al-Salem and Al-Nassar, 2018; Al-Dousari et al., 2020). Hence, this work will perform a detailed techno-economic assessment and optimization for higher capacity wind power plants using a 2 MW rated wind turbine (i.e., the reference wind turbine). This 2 MW turbine is used in the existing 10 MW wind power plant mentioned above.

1.2. Justification for wind power assessment

According to a referenced study (A Al-Dousari et al., 2019), the existing 10 MW wind power plant mentioned earlier achieved near-record monthly capacity factors during its first year of operation, indicating exceptional performance compared to global reports. This highlights the importance of evaluating larger capacities for wind power plants to meet Kuwait's strategic target of 15% renewable energy by 2030. Therefore, this work aims to conduct a comprehensive techno-economic assessment and optimization of wind power plants in Kuwait's arid climate. One of the key objectives is to provide the necessary technical and economic data to maximize renewable energy penetration and support the achievement of the target. Additionally, the chosen location for the study possesses abundant wind and solar resources, making it highly favorable for renewable generation despite minimal existing transmission networks in the area (Alhajraf and Heil, 2011; GENI, 2017; Mirza, 2018; Alnassar et al., 2005; SolarGIS, 2019; Shams et al., 2017). Moreover, this location exhibits low oil and gas field concentrations (Shams et al., 2017; MOO, 2016). As a result, identifying the peak wind resource periods for wind power dispatch scheduling can maximize the capacity factor of future networks. Introducing wind power for electricity generation in Kuwait would also yield economic

advantages compared to the current business-as-usual approach.

1.3. Benefits and applications

To date, there has been limited exploration of wind power technology on a large-scale level to meet Kuwait's ambitious goal of generating 15% of its electricity from renewable sources by 2030, specifically in its challenging arid desert climate. Dust storms, high humidity, and extreme temperatures present unique challenges in this region. Considering the ambitious renewable energy target, this study represents one of the first comprehensive investigations into the feasibility and viability of wind power technology under these conditions. The research provides technical and operational guidelines and economic yield figures, valuable for potential developers and investors looking to promote renewable installations through wind power performance evaluations. Additionally, the study offers recommendations on optimal design configurations and operating conditions for future wind power plants. Multiple objectives are achieved through performance assessments, integration of optimal design parameters/operating conditions, and ground-measured meteorological data.

2. Methodology

2.1. Justification for simulation model selection

Several factors in this study influenced the selection of the System Advisor Model (SAM) software based on the Transient System Simulation (TRNSYS) for wind power performance modeling. These factors include: (i) detailed performance analysis: SAM allows for a comprehensive analysis of wind power performance by considering the entire system through system-level simulation. (ii) Availability of input datasets: The software provides access to input datasets containing design parameters for various wind power plant components. These datasets are essential for accurate modeling and (iii) parametric analyses: SAM enables the execution of many simulations through script and code writing capabilities with multiple programming languages. This facilitates conducting parametric analyses to explore various scenarios. As part of building the methodology of this work, the system components have been determined for the wind power model configurations. Several analyses have justified utilizing SAM software based on TRNSYS simulation. The computational algorithm and control are explained for a comprehensive performance assessment of the wind power technology, among other performance metrics such as LCOE and energy-related parameters concerning the performance of plant subcomponents (Ho, 2008). According to SAM developers (Wagner and Gilman, 2011), the software is based on hourly simulations interacting with performance and financial models to calculate energy outcomes and cash flows while considering the Capital Expenses (CAPEX) and Operating Expenses (OPEX) of a project. SAM allows for exchanging data with external software for further detailed analysis, such as using advanced statistical tools, as in this work's case. Most inputs to the model can be used as parametric variables to investigate the impacts of variations in technical performance and economic indicators, such as LCOE (see Appendix E). SAM uses a performance engine (TRNSYS), which includes customized components, developed at the University of Wisconsin. It should be recognized that TRNSYS is a time-series simulation program that can simulate system component performance, and it is integrated into SAM for faster simulation run time.

2.2. Computational algorithm and control

SAM is demonstrated as a software that handles the comprehensive performance of wind power technologies. In general, total system analysis software(s) evaluate the overall performance metrics (LCOE) and energy outputs depending on detailed processes with information concerning the performance of subcomponents (Ho, 2008). The complex process models in SAM require input parameters (see Appendix E) and distributions for uncertainty and sensitivity analyses obtained from surveys of power plants, operational tests, detailed reviews, and expert judgments. The framework for modeling complex systems relies on passing information from various process models to prioritize modeling and characterization for the objectives that impact the financial and performance metrics. In one study (Trabelsi et al., 2016), the algorithms in SAM for analyzing the components, parameters, and time-dependent inputs are explained. In addition, SAM combines hourly simulation models with performance and economic models to estimate energy output, financial metrics, and cash flows. It includes built-in CAPEX, OPEX, and performance models and can exchange data with external models developed in Microsoft Excel. Furthermore, it can model plant-level simulations since the performance of each of the component models is based on correlations, analytical functions, and factors describing the physical processes. This allows detailed modeling, including spatial and temporal variability within subcomponents. Hence, SAM is selected as one of the analysis tools in this work after surveying numerous software(s).

2.3. Modelling approach

As stated earlier, the study utilizes SAM, and it is essential to note that it relies on TRNSYS for simulations (Wagner and Gilman, 2011). It allows users to input design parameters (see Appendix E) for wind power plants to align with the desired operational philosophy and design conditions. Furthermore, it enables a detailed hourly performance evaluation and provides financial and economic estimations for the project (Ho, 2008; Trabelsi et al., 2016). In addition to its performance evaluation and financial estimation capabilities, it also incorporates dispatch optimization features. These features rely on user inputs for dispatch control algorithms and weekday/weekend schedules. This allows users to analyze the effects of different options on plant performance and economics. Further, it relies on various primary input data to ensure accurate simulations and assessments. One of the essential inputs is the typical meteorological year file, which contains site characteristics such as elevation, latitude, and longitude. This file provides detailed meteorological and resource data in the following format: (i) day of the year, (ii) time in hourly format, (iii) air temperature, (iv) relative humidity, (v) wind speed, (vi) wind direction, (vii) atmospheric pressure, and (vii) wet-bulb temperature. Furthermore, financial parameters such as analysis periods, interest rates, price escalation, and inflation rates are crucial to the model. These parameters enable accurate financial evaluations and assessments within the software. As part of this work, Appendix C provides detailed information on the natural resources and meteorological characteristics consisting of the meteorological data, location characteristics, meteorological characteristics, prevailing conditions, and energy output estimation.

2.4. Parametric analyses

In this work, the following outcomes are provided using detailed analyses: (i) daily profiles for wind speed and α at different height levels, (ii) monthly profiles for wind speed and direction frequencies at reference 2 MW wind turbine's hub height with normal distributions, (iii) statistical results of wind speed in m/s, wind direction in deg (°) unit, ambient temperature in °C unit, and other meteorological data at the reference turbine's hub height, and (iv) Locally Estimated Scatterplot Smoothing (LOESS) regression analyses for the wind resource.

It should be mentioned that the row orientation is a critical parameter in designing a wind farm layout. This work presents 60 optimal configurations with optimal values of wind power plant layout angle (θ_{plant}) based on the lowest LCOE. The wake effect or wake turbulence is an important consideration when planning wind farm layouts, as it can impact the efficiency of turbines located downstream of the wind flow. The technical description of the wind farm model considers wake effect

losses, and the used model provides a tool for optimizing the placement of wind turbines within a wind farm to minimize wake effect losses. The wake effect occurs when wind passes over turbine blades, leading to turbulence and reduced wind speed for subsequent turbines located downstream. The inputs to the model are as follows: (i) number of turbines, row orientation or angle west of north of a line perpendicular to the rows of turbines). This impacts the positioning of turbines in relation to prevailing wind directions and (ii) wind direction distribution (input data about the frequency of wind coming from different directions). In the optimization algorithm the model uses optimization algorithms to suggest potential reconfigurations of turbine layout to minimize wake effects while maximizing power output. The model outputs consist of the following: (i) estimated wake losses in which the model provides an estimate of power losses due to wake effects, (ii) optimal layout, which is a suggested turbine layout to minimize wake losses, (iii) performance metrics, which included an overall efficiency and estimated annual energy production. About the limitations and challenges, the model is based on typical wake behavior, and actual results may vary based on local conditions. Hence, assuming homogeneity in turbine types and sizes does not account for variations in terrain, which can also affect wind flow patterns.

Additionally, several evaluations are performed in this work by varying the number of rows in the wind power plant (N_r) and the wind power plant layout angle (θ_{plant}), which are the primary investigated design parameters. The impact of varying N_r and θ_{plant} on the annual gross energy, LCOE, performance ratio, capacity factor, and wake losses are evaluated for 2220 configurations, including 60 optimal design configurations. The model simulation is performed for 2220 runs from which 60 optimal configurations are identified corresponding to various row configurations (i.e., 1-row, 2-row, 3-row, …, 60-row). It should be mentioned that the optimization and performance assessment includes a techno-economic evaluation in which it is established by examining the effects of the two primary design parameters as follows: (i) N_r is varied from 1 to 60 with an increment of 1 row, and (ii) θ_{plant} is varied from 0 to 360 ° with an increment of 10 °.

The total variations bring the investigated simulation runs to 2220 runs, which are divided into 60 categories as follows: (i) category 1 of 60: (1-row x 0 °), (1-row x 10 °), (1-row x 20 °) …, (1-row x 360 °), (ii) category 2 of 60: (2-row x 0 °), (2-row x 10 °), (2-row x 20 °) …, (2-row x 360 °), … …, and up to, (iii) category 60 of 60: (60-row x 0 °), (60-row x 10 °), (60-row x 20 °) …, 60-row x 360 °).

The detailed monthly performance for the following selected 8 of the 60 optimal configurations of wind power plants is further evaluated. It should be recognized that the optimal configurations have optimal values of θ_{plant} based on the lowest LCOE values: (i) category 1 of 60: the optimal 1-row configuration, (ii) category 2 of 60: the optimal 2-row configuration, (iii) category 3 of 60: the optimal 3-row configuration, (iv) category 4 of 60: the optimal 4-row configuration, (v) category 40 of 60: the optimal 40-row configuration, (vi) category 46 of 60: the optimal 46-row configuration, (vii) category 52 of 60: the optimal 52-row configuration, and (vii) category 58 of 60: the optimal 58-row configuration.

In addition, the frequency profiles for the following 12 assessment parameters are evaluated from January to December: (i) parameter 1 of 12: wind speed in m/s unit at the reference turbine's hub height, (ii) parameter 2 of 12: wind direction in deg (°) unit at the reference turbine's hub height, (iii) parameter 3 of 12: ambient temperature in °C unit at the reference turbine's hub height, (iv) parameter 4 of 12: atmospheric pressure in atm unit at the reference turbine's hub height, (v) parameter 5 of 12 under category 1 of 60: generation of the optimal 1-row configuration in kW unit, (vi) parameter 6 of 12 under category 2 of 60: generation of the optimal 2-row configuration in kW unit, (vii) parameter 7 of 12 under category 3 of 60: generation of the optimal 3-row configuration in kW unit, (vii) parameter 8 of 12 under category 4 of 60: generation of the optimal 4-row configuration in kW unit, (ix) parameter 9 of 12 under category 40 of 60: generation of the optimal 40-row configuration in kW unit, (x) parameter 10 of 12 under category 46 of 60: generation of the optimal 46-row configuration in kW unit, (xi) parameter 11 of 12 under category 52 60: generation of the optimal 52-row in kW unit, and (xii) parameter 12 of 12 under category 58 of 60: generation of the optimal 58-row configuration in kW unit. Furthermore, the Monthly Frequency Profiles (MFPs), Hourly Frequency Profiles (HFPs), and Annual Frequency Profiles (AFPs) for the 12 assessment parameters mentioned above are evaluated.

2.5. Modelling approach

In this work, SAM is used in analyzing wind power performance modeling (Wagner and Gilman, 2011; NREL, 2019). The flexibility of selecting various design parameters is one of the main reasons for selecting it, as it allows the user to set rated design conditions. Additionally, it provides the capability to conduct a thorough hourly performance assessment, allowing for a detailed evaluation of project performance over time. It also offers financial and economic estimations tailored explicitly to the analyzed project. This enables users to assess the project's financial viability and economic feasibility based on various factors and input parameters (Ho, 2008; Trabelsi et al., 2016).

Moreover, SAM encompasses dispatch optimization features that depend on user inputs (see Appendix E) for the dispatch control algorithm, incorporating schedules for weekdays and weekends. This functionality enables users to evaluate the effects on wind power plant performance and economics, offering a range of options for analysis. Furthermore, it takes a comprehensive approach by considering the plant's performance and providing detailed assessments of electricity output. This ensures a comprehensive evaluation of the plant's performance and contribution to the overall electricity generation system (Hamilton et al., 2020; Wagner, 2008). Such features strongly support the use of SAM in project assessments for wind power plants to provide feasibility measures before installation and construction (Fares and Abderafi, 2018; Ashurst, 2016).

Several design parameters must be provided as inputs to run simulations for wind power modeling in SAM. These parameters include wind turbine design details, the type of SRW meteorological file, location characteristics, and financial input parameters. For the simulation model, the meteorological parameters required as inputs are air temperature, relative humidity, wind speed, wind direction, and atmospheric pressure. These parameters are needed for 8760 h yearly, comprehensively representing meteorological conditions. When modeling a mega-scale system like a wind power plant with various subsystems, one of the main challenges is managing the computational demand of the subsystem models; hence, specific techniques are employed to reduce simulation running time. This study considers using software(s) for time-series analyses, which helps mitigate the intensive computational time, especially when conducting detailed parametric analyses. These software tools aid in achieving faster simulations while maintaining accuracy and facilitating detailed analysis of the wind power plant system.

3. Results and discussion

3.1. Technology description

This work presents a comparative techno-economic assessment and minimization of the LCOE for increasing wind power capacity by row and angle layout optimization. In the wind power plants, each wind turbine within the designated rows has a rated capacity of 2 MW, the standard capacity for the reference wind turbine mentioned earlier. Additionally, reference 2 MW wind turbine has a cut-in wind speed of 3 m/s, a rated wind speed of 11 m/s, and a cut-out wind speed of 25 m/s. These wind speed thresholds determine the operational range of the turbine, indicating the wind speeds at which it starts generating power,

operates at its rated capacity, and shuts down to protect itself from excessive winds. Fig. 1 shows a simplified illustration for a single-row configuration to be used as the base for analyzing 2220 design configurations. These configurations have increasing power capacities and are connected to the following components: (i) electrical grid, (ii) substations (step-up/down), (iii) overhead lines, and (iv) residential units. Fig. 2 shows reference 2 MW wind turbine's power curve, and Table 1 shows its design characteristics used in this work. It should be recognized that the design characteristics for the wind turbine type used in this work are shown in Table 1.

The reference 2 MW wind turbine has specific technical specifications and service requirements as a large-scale wind turbine. The turbine's mechanical design considers enhanced mechanical capacity in various components, including the yaw system, framework, central axis, and blade bearings. These improvements aim to increase the turbine's component reliability and enable larger rotors' utilization. The larger rotor size allows for capturing more wind kinetic energy, maximizing power generation even in varying wind strengths. The turbine aims to improve overall performance and efficiency by optimizing these aspects. Additionally, in the turbine's drive train, the main axis is supported by two spherical bearings, which offer added advantages. These bearings help transmit the surrounding loads to the framework through a rack, preventing the gearbox from experiencing additional loads. This design feature helps to reduce breakdowns and extends the overall lifespan of the turbine. Minimizing stress on the gearbox allows the turbine to operate more efficiently and reliably, resulting in improved performance and durability. Furthermore, the turbine's design includes a lightning protection system that adheres to the International Electrotechnical Commission (IEC) 62,305 standard. This system is implemented to prevent lightning strikes from causing damage to the turbine. The lightning protection system conducts the lightning from the sides of the blade's tip to the root, through the nacelle, tower structure, and ultimately into the foundation (ground). This protection mechanism safeguards the blades, bearings, and main axis from the potentially harmful effects of lightning traveling through them. Also, it helps prevent burnout situations for the electrical and electronic equipment within the turbine. Moreover, the turbine is equipped with a controlled braking system. This includes aerodynamic brakes and mechanical emergency brakes located at the output of the high-speed axis of the gearbox. These brakes ensure that the turbine can be safely stopped when needed. A hydraulic control system is also incorporated to provide braking in cases of excessive transmission load, further enhancing the safety and control of the turbine's operation.

3.2. Mathematical description

Several factors play a crucial role in determining the performance of wind power-generating units (Aeolos, 2020). Among these factors, wind speed is considered the primary and most influential factor when estimating the energy output of a unit. Eq. (1) illustrates the relationship between wind speed and energy output. Wind speed plays a crucial role

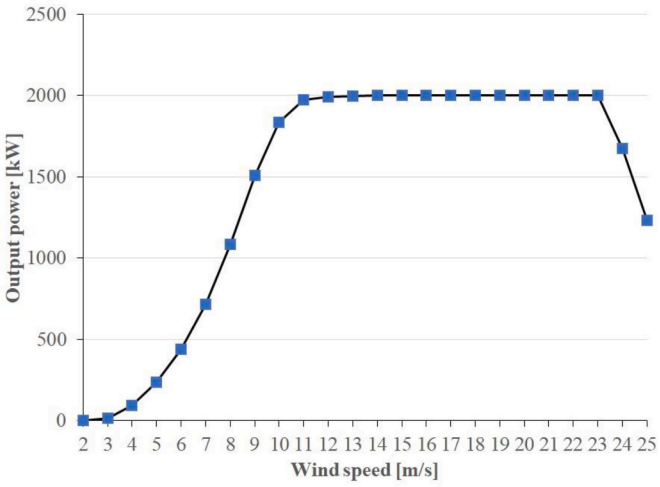

Fig. 2. Power curve for reference 2 MW wind turbine used in this work.

as it directly affects the rotation speed of a wind turbine's blades. Higher wind speeds lead to faster blade rotation, resulting in increased energy production compared to situations with lower wind speeds. The relationship between wind speed and energy production is such that higher wind speeds translate into higher power output from the wind turbine. The output of the wind power-generating unit (P_w) is determined using Eq. (1), commonly known as Betz's law. The equation describing the relationship between wind energy extraction and the principles of mass and momentum conservation is derived from the theoretical concept known as Betz's law. A German physicist, Albert Betz, formulated this law in 1919 to establish the maximum achievable energy capture from wind, independent of specific wind turbine designs. According to Betz's law, no turbine can capture more than 59.3% of the available energy in the wind at a given location. This value, expressed as the fraction 16/27 or approximately 0.593, is commonly referred to as Betz's coefficient (see Appendix D).

$$P_w = (1/2) C_p \rho A_b u_h^3 \quad (1)$$

where C_p is the wind turbine power coefficient or performance coefficient (i.e., an indicator of turbine efficiency), ρ is the air density, A_b is the blade's swept area of the turbine, and u_h is the wind speed at the turbine's hub height.

Several factors influence the performance of wind power-generating units. The second factor is the parameter α, which relates to the unit's wind speed and installation height. The optimal hub height for installation depends on the α value. If α is significant, it can cause an imbalance in the wind load on the blades' swept area, adversely affecting both the blades and the nacelle. This imbalance can result in operational problems and a shorter lifespan for the unit. The third important factor is the ambient temperature. When the ambient temperature exceeds the

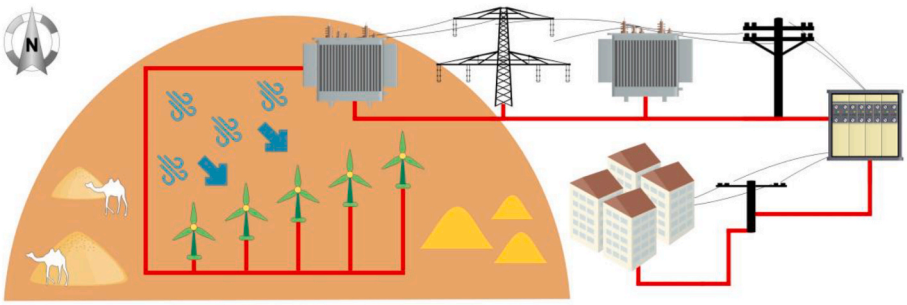

Fig. 1. Simplified illustration of a single-row configuration with grid connection, substations, overhead lines, and residential units.

Table 1
Design characteristics for the reference wind turbine used in this work.

Description	Value	Unit
Make and model	Siemens-Gamesa G97	–
Power capacity	2000	kW
Number of blades	3	–
Cut-in wind speed	3	m/s.
Rated wind speed	11	m/s.
Cut-out wind speed	25	m/s.
Rotor diameter	97	m
Swept area	7390	m^2
Rotational speed	9.6–17.8	rpm
Blade material	pre-impregnated epoxy glass fiber + carbon fiber	–
Blade length	47.5	m
Blade cord, maximum	3,41	m
Blade cord, minimum	0,057	m
Blade torsion	8,5	m
Turbine cover dimensions	10.583 × 3505 × 4487	m
Turbine cover material	reinforced matrix composite	–
Turbine hub material	Nodular cast iron	–
Main shaft type	Cast shaft	–
Main shaft support	Nodular cast iron	–
Front frame material	Nodular cast iron	–
Yaw system type	Yaw ring with friction bearing	–
Tower type	Tubular truncated	–
Tower material	Structural carbon steel	–
Tower surface treatment	Painted	–
Gearbox type	1 planetary stage, 2 parallel stages	–
Gearbox ratio	1:106.8 (50 Hz) 1:127.1 (60 Hz)	–
Main shaft coupling	Cone collar	–
High-speed shaft coupling	Flexible coupling	–
Generator type	Doubly-fed machine	
Generator nominal power	2070	kW
Generator voltage	690	Vac
Generator frequency	50/60	Hz
Mechanical brake type	Disc	–
Hydraulic unit operating pressure	220	bar
Control unit voltage	24	Vdc
Transformer type	Three-phase, dry-type encapsulated	–
Nacelle weight	72	t
Rotor weight	47	t
Tower weight	165	t

normal operating range of the unit, it has a noticeable impact on the energy output. Higher temperatures lead to a decrease in air density, which decreases the energy output, according to Eq. (1). Shallow ambient temperatures can also cause the blades to freeze, necessitating a shutdown of the unit. The fourth factor is the tower height on which the wind power-generating unit is mounted. As the tower height increases, the unit's energy output increases due to higher wind speeds at greater heights above the ground. The air density is the fifth-factor affecting energy output estimation, as indicated in Eq. (1). Lower air density corresponds to weaker winds, increasing the unit's rated wind speed and cut-in speed, thereby reducing the energy output. The sixth factor is the unit's rated capacity, which refers to the maximum power the generator can produce. A lower rated capacity corresponds to a lower annual energy output. Lastly, the seventh factor is the yearly valid operating period. A shorter active working period leads to a smaller annual energy output. It is important to note that periods of zero production are considered when calculating the capacity factor. Therefore, accurately estimating the unit's availability in a large-scale power plant is crucial as it directly impacts the project's economic feasibility.

To achieve the best possible effectiveness, upholding the designated power export to the grid is generally advised. The economic viability of a wind power facility can be assessed through various means, with the LCOE method being the most commonly employed approach. This method considers the CAPEX and OPEX of installation, electricity generation, and operational and maintenance expenditures, thereby offering a thorough economic evaluation. The LCOE criterion is extensively used in scholarly works to compare diverse electricity generation technologies (Branker et al., 2011; IRENA, 2012; Hoffmann, 2010; IRENA, 2018). The LCOE method determines the net present value of the electricity's unit cost over the entire lifespan of a thermal power generation unit. It estimates the price the technology needs to attain to recover expenses and reach a breakeven point throughout the plant's operational period (IRENA, 2012). In this work, the LCOE is calculated using Eq. (2) as follows (Short et al., 1995):

$$\mathrm{LCOE} = \frac{\mathrm{FCRxTCC} + \mathrm{FOC}}{\mathrm{AEP}} + \mathrm{VOC} \tag{2}$$

where,

FCR: Fixed Charge Rate is the revenue per amount of investment required to cover the investment cost (−).
TCC: Capital cost or installed capital costs (CAPEX) ($).
FOC: Fixed annual operating cost or operations and maintenance costs (OPEX) ($).
VOC: Variable operating cost or operations and maintenance costs per unit of annual electricity production ($/kWh).
AEP: Annual Electricity Production (kWh).

In one study (Mohideen et al., 2023), the cost of hydrogen is analyzed. For simplicity, extending that understanding to electricity production provides a preliminary idea of the financial analysis of LCOE. For instance, the cost of electricity is measured using the metric LCOE, which can be thought of for simplicity purposes to illustrate the discounted lifespan cost of installing and maintaining a plant or as cost per energy unit of electricity production. Hence, LCOE can be thought of preliminary as the ratio of the net present value of the total cost of the electricity production plant to the net production value of the total quantity of electricity anticipated to be generated during the plant's lifetime, as shown in Eq. (3), Eq. (4) and Eq. (5) where n is a time period.

$$\text{Net present value of total cost} = \sum_{n} \frac{\text{Total CAPEX and OPEX}_n}{(1 + \text{discount rate})n} \tag{3}$$

$$\text{Net present value of electricity product} = \sum_{n} \frac{\text{Electricity Production}_n}{(1 + \text{discount rate})n} \tag{4}$$

$$\mathrm{LCOE} = \sum_{n} \frac{\text{Net present value of total cost}}{\text{Net present value of electricity product}} \tag{5}$$

According to the IEC standard 61,400–1, wind power plant locations are categorized into different classes of wind turbines based on the wind resource characteristics. These characteristics include mean wind speed at the turbine's hub height, average turbulence intensity, gust wind speeds, and the wind shear parameter α. Wind turbines experience static and dynamic loads from various sources, including. This standard specifies limitations on α and defines allowable ranges. The design limit for α is set at 0.2, meaning that locations with α values above 0.2 are generally considered undesirable for most wind turbine classes. This indicates that an excessive value of α can pose challenges and may not be suitable for wind turbines' efficient and reliable operation.

Once the Reference Level of Calculations (RLCs) is determined, the wind speed data collected from a meteorological mast at the selected location in Kuwait is utilized to calculate the α values. Detailed 10-min analyses specifically focus on α between two elevations: 100 m and 40 m. The mean, maximum, minimum, and total number of α values are evaluated. These assessments provide valuable insights into the characteristics of α at the site, shedding light on the wind shear parameter's behavior and variability within the studied area. Using Eq. (6), the annual mean of α, calculated within the range of 0.14–0.18, is crucial in estimating the wind energy yield at the chosen location. These

calculations play a significant role in accurately assessing the wind resource potential and predicting the energy output from the wind power plant. An accurate estimation of α is essential for evaluating the potential wind energy generation at the site. It helps in determining the appropriate wind turbine design, optimizing the performance of the wind power plant, and making informed decisions regarding project feasibility and profitability.

$$\alpha = \frac{\ln(u_2/u_1)}{\ln(z_2/z_1)} \tag{6}$$

where u_1 is the wind speed at a higher altitude, u_2 is the wind speed at a lower altitude, z_1 is the higher altitude, and z_2 is the lower altitude. It is essential to acknowledge that in the selected location for this study, the atmosphere tends to be relatively stable during nighttime. This stability contributes to a noticeable shear in the boundary layer. The shear refers to a variation in wind speed and direction with height; in this case, it becomes more prominent during nighttime due to the atmosphere's stability. It is worth noting that the observed cyclic trend of the wind resource can serve as a compensatory factor for afternoon peak load shaving or leveling in Kuwait. Consequently, this trend of having a pronounced shear in the boundary layer during nighttime can potentially enhance wind power generation and the Peak Load Shaving Capability (PLSC). The PLSC refers to the ability of a wind power plant to reduce peak electricity demand. It can be estimated using Eq. (7) as follows:

$$\mathrm{PLSC} = \sum_{y=1}^{k} E(N_h^{cr}) \Big/ N_h^{cr} \tag{7}$$

where $E(N_h^{cr})$ is the amount of electricity produced by a renewable power technology, such as wind power, and N_h^{cr} is the number of critical hours. Additionally, the output of a single wind power-generating unit (P_w) is calculated from Eq. (8). Furthermore, the wind power density (P_d) is calculated using Eq. (8) (see Appendix D).

$$P_d = (1/2)\rho u_h^3 \tag{8}$$

3.3. Wind resource, statistical, and regression analyses

Fig. 3 shows the hourly wind speed and α profiles for one day in the chosen location in Kuwait at different height levels. The comparison between daytime and nighttime reveals that the difference in the vertical α is noticeable. The wind speeds are distributed equally and vertically during the day with lower α values (on average, $\alpha = 0.15$). In comparison, the wind speeds increase for higher elevations above the ground at night, thus increasing the α values ($\alpha > 0.29$).

It should be noted that understanding wind behavior and class is crucial for assessing the chosen location's suitability for mega-scale wind power installations since mega-scale wind turbines are designed to withstand certain design conditions. Considering a mean air density of 1.12 kg/ m^3, a rotor-swept area of 7390 m^2 for the reference wind turbine with a rated capacity of 2 MW, a rotor diameter of 97 m, and a mean wind speed of 8.02 m/s (as shown in Table 1); therefore, the P_d value is calculated to be 289 W/ m^2 using Eq. (8) (see Appendix D).

Generally, an annual frequency evaluation of wind speed and direction is insufficient for wind power assessment. Therefore, the corresponding monthly profiles have been investigated in this work. A detailed resource assessment focusing on wind speed and direction has also been performed for the chosen location in Kuwait. The evaluation resulted in identifying wind dominance in the northwest direction. It can be concluded that June and July have maximum wind speed profiles and dominant wind direction with consistent two levels compared to other months, showing relative dominance in the same wind direction.

In particular, the wind resource assessment incorporated several regression analyses of LOESS. This work utilizes the LOESS regression method to find the best fit for the wind data points. It should be recognized that the LOESS analysis is an investigation in which least squares regression is performed in localized subsets, such as in the case of hourly wind speed and wind direction data. The complete LOESS analyses concluded that the wind direction and distribution ranges showed consistent and robust northwest components. In addition, the seasonal wind direction distribution is evaluated, and the dominant wind direction is observed to be maintained without significant variations throughout the year (see Figs. 4–6). Fig. 4 shows various plots corresponding to separate monthly LOESS analyses. It should be noted that the horizontal axes in Fig. 4 indicate the wind direction in the deg

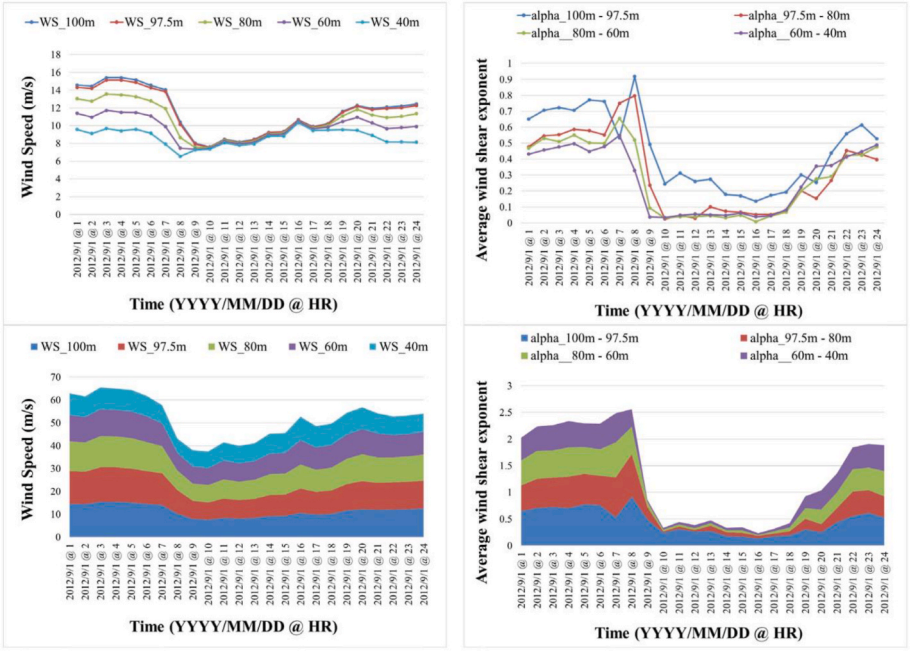

Fig. 3. Profiles for the wind speed and α at different height levels during one day.

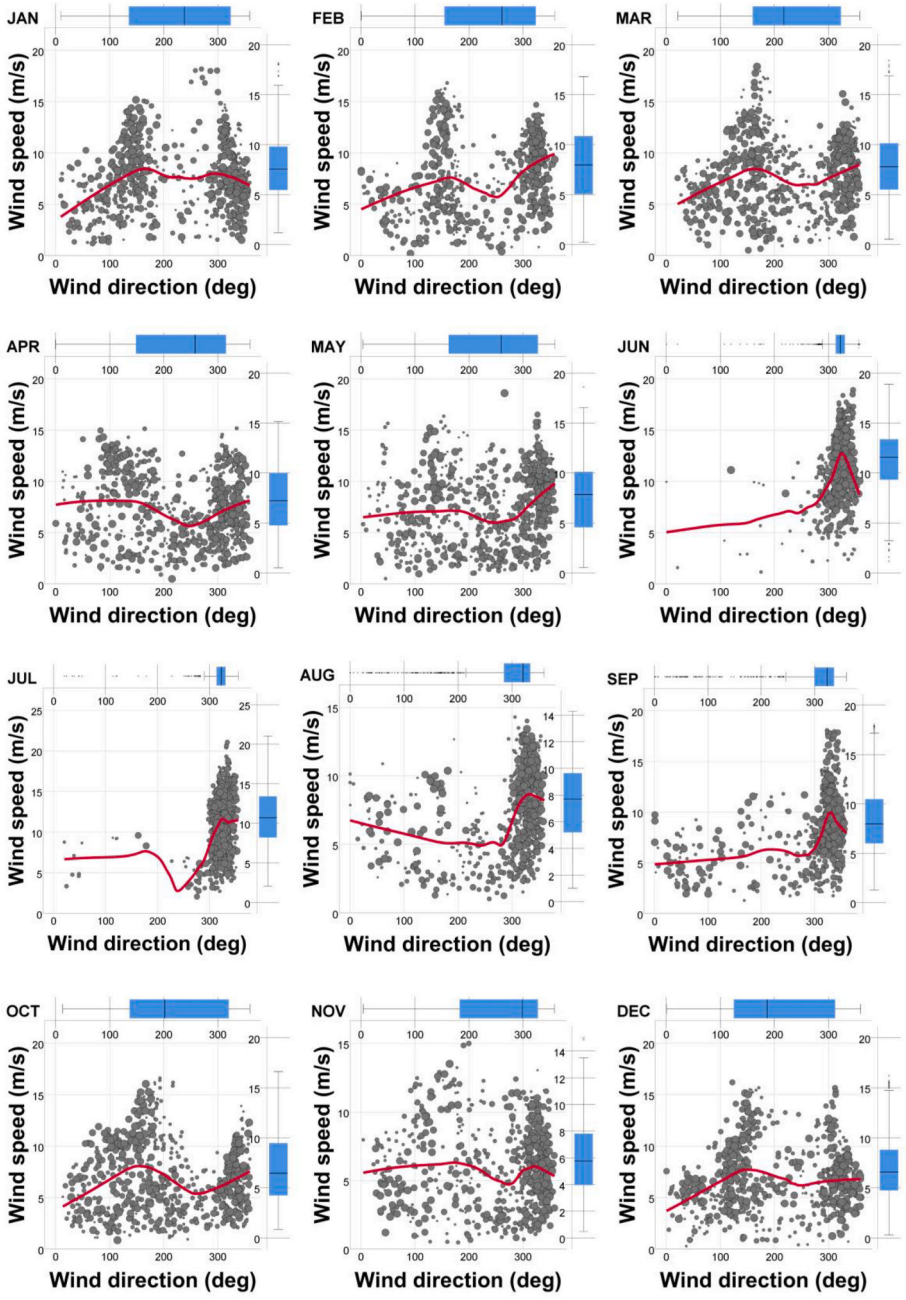

Fig. 4. Results of the LOESS regression analyses (monthly) for the wind resource during hours 0 to 23 for a typical year in the chosen location in this work.

(°) unit, whereas the vertical axes indicate the wind speed in the m/s unit. The boxplots on the right and top sides of the plots provide helpful information concerning the range, average, maximal, and minimal values.

In statistical modeling, a regression analysis is a set of statistical processes for estimating the relationship between a dependent variable and other independent variables (one or more). The LOESS regression analyses reveal that the correlations between wind speed and direction provide essential information for identifying the months with the highest contribution toward wind power generation. Hence, such findings can be used in wind power scheduling to increase the energy yield of future mega-scale installations of wind power plants (i.e., high power capacities) in the chosen location in Kuwait. As illustrated in Fig. 4, the large markers represent the hour count in which the early hours of the day are represented with smaller markers than later. Furthermore, the wind speed and direction correlations show consistent trends in June, July, August, and September. Thus, it is revealed that a high concentration exists at a specific wind direction, i.e., approximately 318 °. Additionally, it is concluded that the highest concentrations occur during June and July, with a mean wind speed of 11.27 m/s and 10.74 m/s, respectively. Further, as shown in Fig. 4, the red curves indicate sharp spikes at approximately 318 °, confirming the previous finding. Table 2 shows statistical results (annual) for the primary meteorological data at the reference wind turbine's hub height. It is crucial to understand the wind resource if despatching wind power is accompanied by other renewable energy technologies, such as CSP-PT. Also, CSP-PT with TES capability is considered a dispatchable power source and can provide additional economic benefits once combined with wind power, an intermittent source. For the chosen location in Kuwait, it is essential to realize that the wind resource is at maximal levels during the nighttime when CSP-PT can be dispatched using a TES system. Such dispatch operation will increase the economic feasibility and reduce the

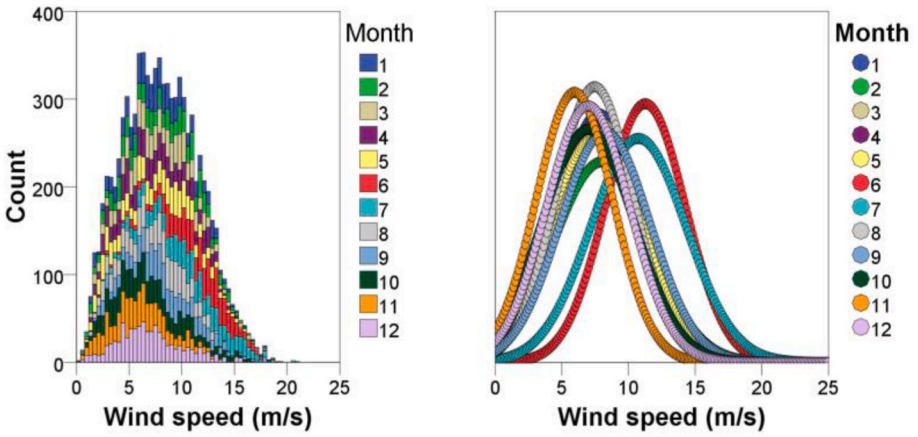

Fig. 5. Monthly profiles for the wind speed frequency (left) at the reference wind turbine's hub height with normal distributions (right).

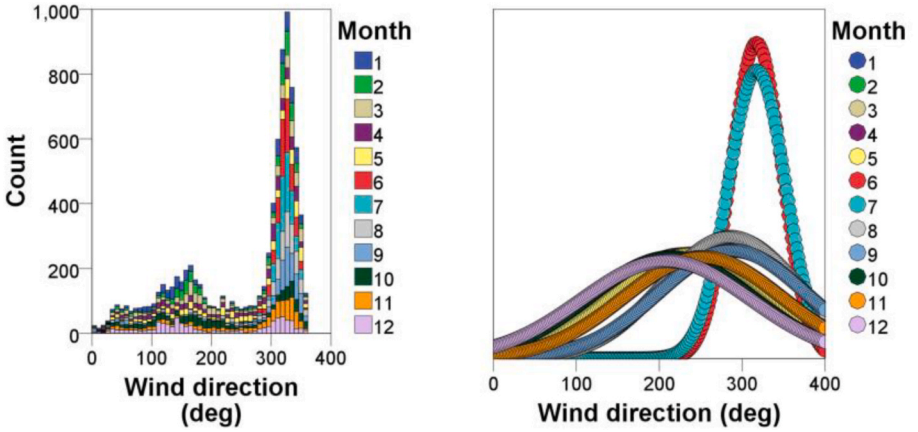

Fig. 6. Monthly profiles for the wind direction frequency (left) at the reference wind turbine's hub height with normal distributions (right).

Table 2
Statistical results (annual) for primary meteorological data at the reference wind turbine's hub height during a typical year.

Description	Wind speed, (m/s)	Wind direction, (°)	Atmospheric pressure, (atm)	Ambient temperature, (°C)
Mean	8.02	253.30	0.9646	30.89
Median	7.85	306.11	0.9654	31.98
Maximum	21.05	359.91	0.9832	50.20
Minimum	0.22	0.24	0.9493	7.88
Range	20.83	359.67	0.0339	42.32
Standard Deviation	3.59	95.73	0.0067	9.78

curtailment of renewable power cogeneration. It should be recognized that the wind resource assessment and the LOESS regression analyses have provided an acceptable correlation between wind speed and direction, resulting in the nighttime showing maximal values. Therefore, CSP-PT and wind power complement each other for the case of the chosen location in this work, as shown in Table S. 9 (solar resource) and Figs. 4–6 (wind resource).

3.4. Optimization analyses

In this work, the model simulation is performed for 2220 design configurations, from which 60 optimal configurations are identified corresponding to different row configurations. The optimization is accompanied by a techno-economic evaluation, which is established by studying the effects of varying two primary parameters (N_r and θ_{plant}) for several wind power plants using reference 2 MW wind turbine. The variations bring the total investigated simulations to 2220 runs, divided into 60 categories. While interpreting the following sections, it should be noted that the results of the 2220 configurations are shown in three-dimensional (3D) illustrations, i.e., Fig. 7(a and b), Fig. 8(a and b), Fig. 9(a and b), and Fig. 10(a and b). Whereas the 60 optimal configurations (one for each of the 60 categories as mentioned earlier) are shown in two-dimensional (2D) illustrations, i.e., Figs. 7(c), 8(c) and 9 (c), and Fig. 10(c).

The impact of varying N_r and θ_{plant} on the LCOE, and annual gross energy is evaluated. Fig. 7(a) shows the results of a parametric analysis, which reveals that the change in the LCOE occurs as the N_r and θ_{plant} values differ. As the N_r value increases, an increase in the LCOE occurs for the following ranges of θ_{plant}: 110-140 ° and 280-320 ° (red areas). Whereas at small values of N_r, a decrease in the LCOE occurs for the following ranges of θ_{plant}: 0-75 °, 160-260 °, and 340-360 ° (dark-blue areas). Fig. 7(b) shows a linear increase in annual gross energy as the N_r value increases for almost all ranges of θ_{plant}. Fig. 7(c) shows the LCOE, N_r, and θ_{plant} for each of the 60 optimal configurations based on the LCOE-minimization criterion.

The impact of varying N_r and θ_{plant} on the wake losses and annual gross energy is evaluated. Fig. 8(a) shows the results of a parametric analysis, which reveals that the change in the wake losses occurs as the N_r and θ_{plant} values differ. As the N_r value increases, an increase in the wake losses occurs for the following ranges of θ_{plant}: 110-140 ° and 280-320 ° (red areas). Whereas at small values of N_r, a decrease in the wake losses occurs for the following ranges of θ_{plant}: 0-75 °, 160-260 °, and

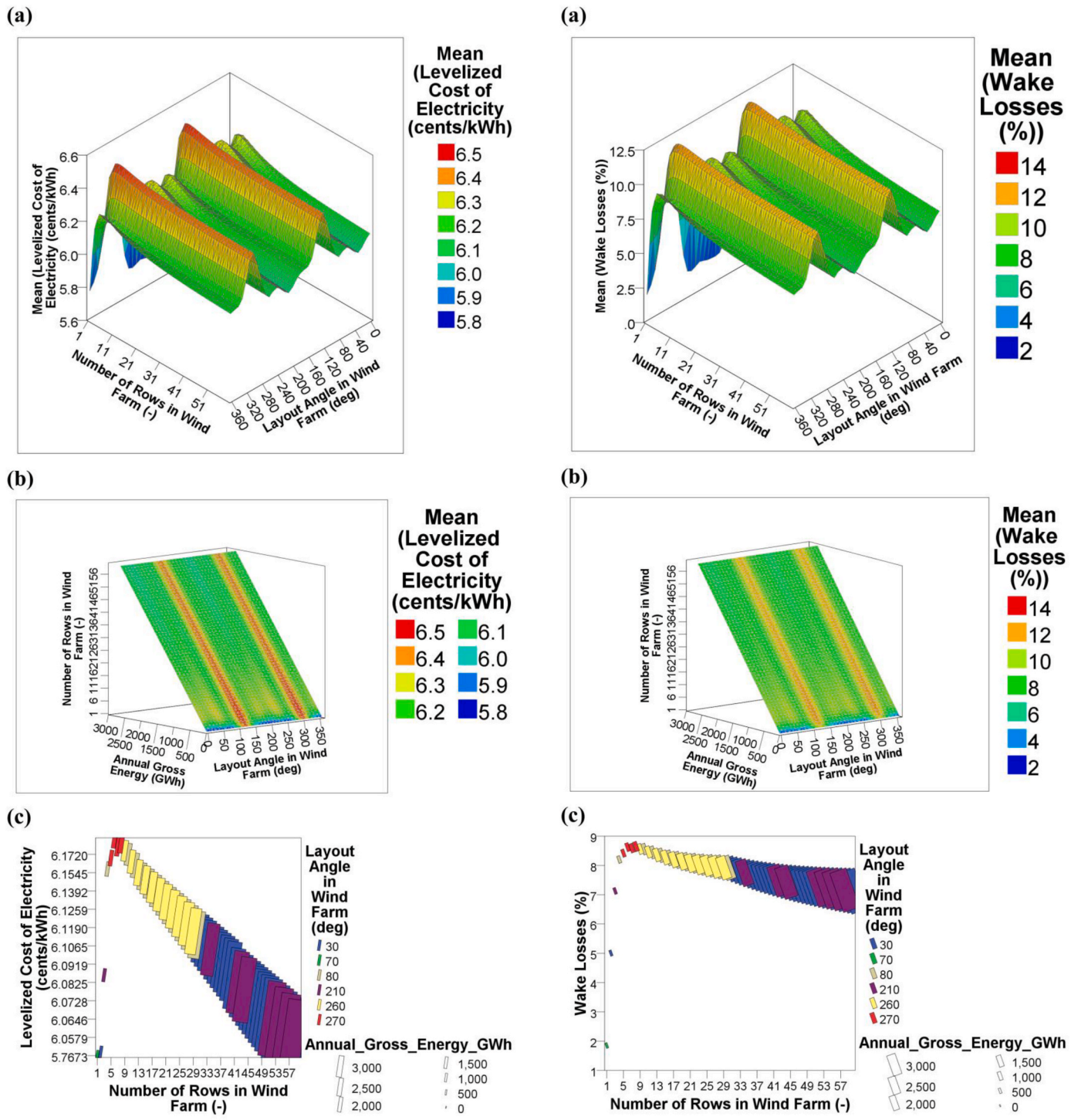

Fig. 7. Impact of varying N_r and θ_{plant} on the LCOE and annual gross energy: (a) for 2220 configurations, (b) for 2220 configurations, and (c) for 60 optimal configurations.

Fig. 8. Impact of varying N_r and θ_{plant} on the wake losses and annual gross energy: (a) for 2220 configurations, (b) for 2220 configurations, and (c) for 60 optimal configurations.

340-360 ° (dark-blue areas). Fig. 8(b) shows a linear increase in annual gross energy as the N_r value increases for almost all ranges of θ_{plant}. Also, Fig. 8(c) shows the wake losses, N_r, and θ_{plant} for each of the 60 optimal configurations based on the LCOE-minimization criterion.

The impact of varying N_r and θ_{plant} on the performance ratio and annual gross energy is evaluated. Fig. 9(a) shows the results of a parametric analysis, which reveals that the change in the performance ratio occurs as the N_r and θ_{plant} values differ. As the N_r value increases, a decrease in the performance ratio occurs for the following ranges of θ_{plant}: 110-140 ° and 280-320 ° (dark-blue areas). Whereas at small values of N_r, an increase in the performance ratio occurs for the following ranges of θ_{plant}: 0-75 °, 160-260 °, and 340-360 ° (red areas). Fig. 9(b) shows a linear increase in annual gross energy as the N_r value increases for almost all ranges of θ_{plant}. Also, Fig. 9(c) shows the performance ratio, N_r, and θ_{plant} for each of the 60 optimal configurations based on the LCOE-minimization criterion.

The impact of varying N_r and θ_{plant} on the capacity factor and annual gross energy is evaluated. Fig. 10(a) shows the results of a parametric

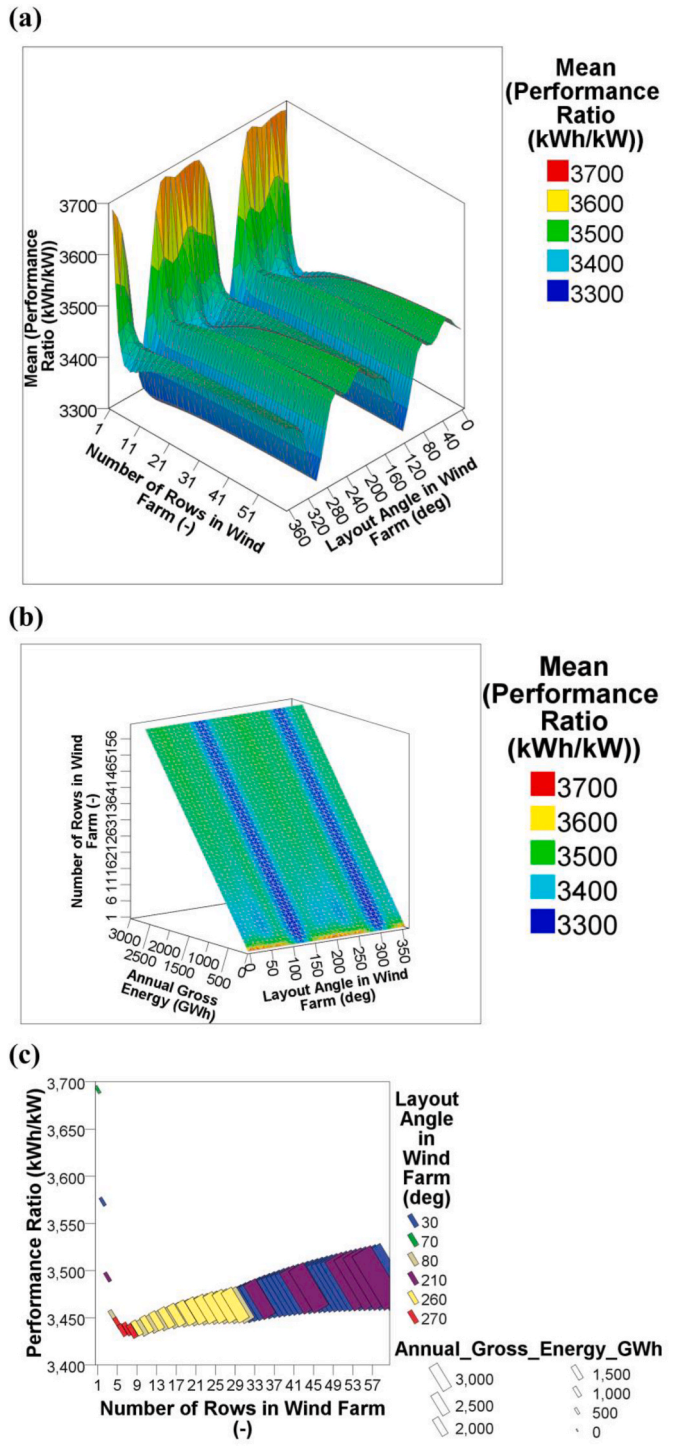

Fig. 9. Impact of varying N_r and θ_{plant} on the performance ratio and annual gross energy: (a) for 2220 configurations, (b) for 2220 configurations, and (c) for 60 optimal configurations.

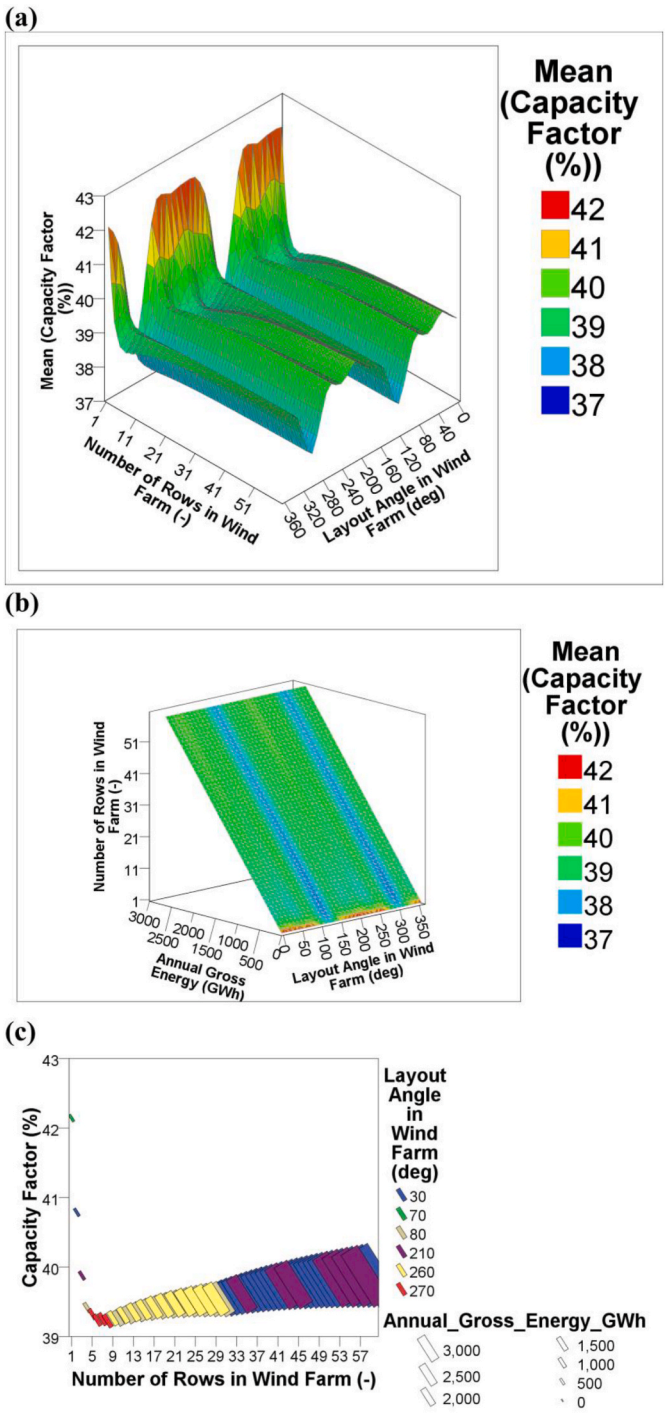

Fig. 10. Impact of varying N_r and θ_{plant} on the capacity factor and annual gross energy: (a) for 2220 configurations, (b) for 2220 configurations, and (c) for 60 optimal configurations.

analysis, which reveals that the change in the capacity factor occurs as the N_r and θ_{plant} values differ. As the N_r value increases, a decrease in the capacity factor occurs for the following ranges of θ_{plant}: 110-140 ° and 280-320 ° (dark-blue areas). Whereas at small values of N_r, an increase in the capacity factor occurs for the following ranges of θ_{plant}: 0-75 °, 160-260 °, and 340-360 ° (red areas). Fig. 10(b) shows a linear increase in annual gross energy as the N_r value increases for almost all ranges of θ_{plant}. Also, Fig. 10(c) shows the capacity factor, N_r, and θ_{plant} for each of the 60 optimal configurations based on the LCOE-minimization criterion.

3.5. Impact of wind resource

Firstly, Figs. 5–7 reveal that the frequency of the wind resource has a clear impact on the LCOE and annual gross energy once linked with the variation of N_r and θ_{plant}. Because there are more wind turbines for higher N_r values, the turbines create more turbulence at high wind speeds, leading to increased wake losses. As a result, the generation decreases, and the LCOE rises accordingly. This explanation justifies the continuous increase in the LCOE shown in Fig. 7(a) for θ_{plant}: 110-140 ° and 280-320 ° (red areas). Furthermore, this explanation justifies the

initial slight increase and continuous decrease in the LCOE for θ_{plant}: 0-75 °, 160-260 °, and 340-360 ° (dark-blue areas). Secondly, Figs. 5–7 and 8 reveal that the frequency of the wind resource has a clear impact on the wake losses and annual gross energy once linked with the variation of N_r and θ_{plant}. Because there are more wind turbines at higher N_r values, the turbines create more turbulence at high wind speeds, leading to increased wake losses. As a result, the generation decreases, and the wake losses increase accordingly. This explanation justifies the continuous increase in the wake losses shown in Fig. 8(a) for θ_{plant}: 110-140 ° and 280-320 ° (red areas). Furthermore, this explanation justifies the initial slight increase and continuous decrease in the wake losses for θ_{plant}: 0-75 °, 160-260 °, and 340-360 ° (dark-blue areas). Thirdly, Figs. 5–7 and 9 reveal that the frequency of the wind resource has a clear impact on the performance ratio and annual gross energy once linked with the variation of N_r and θ_{plant}. Because there are more wind turbines for higher N_r values, the turbines create more turbulence at high wind speeds, leading to increased wake losses. As a result, the generation decreases, and the performance ratio drops accordingly. Lastly, Figs. 5–7 and 10 reveal that the frequency of the wind resource has a clear impact on the capacity factor and annual gross energy once linked with the variation of N_r and θ_{plant}. Because there are more wind turbines for higher N_r values, the turbines create more turbulence at high wind speeds, leading to increased wake losses. As a result, the generation decreases, and the capacity factor decreases accordingly.

3.6. Monthly performance assessment

This section evaluates the Monthly Frequency Profiles (MFPs) of the selected 8 of the 60 optimal configurations (i.e., for categories 1, 2, 3, 4, 40, 46, 52, and 58 of 60) in relation to the Annual Frequency Profiles (AFPs). The optimal selection is based on the LCOE-minimization criterion, and the selected eight optimal configurations are as follows: (i) the optimal 1-row configuration at 70 ° ($N_r = 1$ and $\theta_{plant} = 70$ °), (ii) the optimal 2-row configuration at 30 ° ($N_r = 2$ and $\theta_{plant} = 30$ °), (iii) the optimal 3-row configuration at 210 ° ($N_r = 3$ and $\theta_{plant} = 210$ °), (iv) the optimal 4-row configuration at 80 ° ($N_r = 4$ and $\theta_{plant} = 80$ °), (v) the optimal 40-row configuration at 30 ° ($N_r = 40$ and $\theta_{plant} = 30$ °), (vi) the optimal 46-row configuration at 30 ° ($N_r = 46$ and $\theta_{plant} = 30$ °), (vii) the optimal 52-row configuration at 210 ° ($N_r = 52$ and $\theta_{plant} = 210$ °), and (vii) the optimal 58-row configuration at 210 ° ($N_r = 58$ and $\theta_{plant} = 210$ °).

It should be recognized that the MFPs of the 12 assessment parameters are shown in Fig. S. 31 to Fig. S. 34 for the January to December months. Additionally, the 12 parameters are listed in the following order from left to right in Fig. S. 31 to Fig. S. 34: (i) wind speed, (ii) wind direction, (iii) ambient temperature, (iv) atmospheric pressure, (v) generation of run 421 of 2220: "the optimal 1-row configuration", (vi) generation of run 182 of 2220: "the optimal 2-row configuration", (vii) generation of run 1263 of 2220: "the optimal 3-row configuration", (vii) generation of run 484 of 2220: "the optimal 4-row configuration", (ix) generation of run 220 of 2220: "the optimal 40-row configuration", (x) generation of run 226 of 2220: "the optimal 46-row configuration", (xi) generation of run 1312 of 2220: "the optimal 52-row configuration", and (xii) generation of run 1318 of 2220: "the optimal 58-row configuration".

For each of the 12 assessment parameters, the following applies concerning Fig. S. 31 to Fig. S. 34: (i) the white areas represent the MFPs, (ii) the dark-blue areas represent the AFPs, and (iii) the light-blue areas represent the intersection areas. Firstly, to understand the MFPs illustrations for the 12 assessment parameters, the ambient temperature parameter (parameter 3 of 12) is chosen. It should be noted that since the summer months have higher temperatures than the winter months, the white areas travel from left to right, then from right to left, starting from January and ending in December. This visual understanding should aid in interpreting the data of the MFPs for the 12 parameters, which are shown in Fig. S. 31 to Fig. S. 34. Secondly, the following can be observed from Fig. S. 31 to Fig. S. 34 concerning the wind speed (parameter 1 of 12) profiles: (i) June and July have a wide range of high wind speeds, (ii) October, November, and December have a narrow range of low wind speeds, and (iii) the remaining months have mid-range wind speeds close to the annual average. Thirdly, after considering the results of the LOESS regression analyses for the wind resource (see Fig. 4) along with the MFPs (see Fig. S. 31 to Fig. S. 34), the following can be observed concerning the wind direction (parameter 2 of 12) profiles: (i) June, July, August, and September have concentrated range wind direction close to 318 ° with high wind speeds, and (ii) the remaining months have scattered range wind direction at low and high wind speeds. Fourthly, the following can be observed from Fig. S. 31 to Fig. S. 34 concerning the atmospheric pressure (parameter 4 of 12) profiles, the frequency pattern of the atmospheric pressure is opposite to the ambient temperature (parameter 3 of 12). Finally, the following can be observed from Fig. S. 31 to Fig. S. 34 concerning parameters 5, 6, 7, 8, 9, 10, 11, and 12 of 12 (generation of the optimal 1, 2, 3, 4, 40, 46, 52, and 58-row configuration, respectively): (i) for January and March: the MFPs slightly match the AFPs at the lowest and highest (full load) generation ranges. Also, the MFPs exceed the AFPs in the majority of the moderate generation ranges, (ii) for February: the MFPs exceed the AFPs at the highest generation (full load) range, (iii) for April to May: the MFPs slightly match the AFPs at the highest (full load) generation range and the majority of the moderate generation ranges. Additionally, the MFPs exceed the AFPs at the lowest generation range, (iv) for June to July: the MFPs exceed the AFPs at the highest (full load) generation range and upper-moderate generation ranges, (v) for August: the MFPs exceed the AFPs in the majority of the moderate generation ranges. Moreover, the MFPs perfectly match the AFPs at the lowest generation range, (vi) for September: the MFPs perfectly match the AFPs at the highest (full load) generation range. Additionally, the MFPs exceed the AFPs in the majority of the moderate generation ranges. Also, the MFPs slightly match the AFPs at the lowest generation range, (vii) for October to December: the MFPs exceed the AFPs at the lowest generation range,

3.7. Hourly performance assessment

This section evaluates the Hourly Frequency Profiles (HFPs) of the selected 8 of the 60 optimal configurations (i.e., for categories 1, 2, 3, 4, 40, 46, 52, and 58 of 60) in relation to the Annual Frequency Profiles (AFPs). The optimal selection is based on the LCOE-minimization criterion, and the selected eight optimal configurations are previously explained in Section 3.6 (Monthly performance assessment). It should be recognized that the HFPs of the 12 assessment parameters are shown in Fig. S. 35 to Fig. S. 42 for the 00:00 to 23:00 h in the same order explained in the section above. For each of the 12 parameters, the following applies concerning Fig. S. 35 to Fig. S. 42: (i) the white areas represent the HFPs, (ii) the dark-red areas represent the AFPs, and (iii) the light-red areas represent the intersection areas. Firstly, to understand the HFPs illustrations for the 12 assessment parameters in Fig. S. 35 to Fig. S. 42, the ambient temperature parameter (parameter 3 of 12) is chosen. It should be recognized that since most day hours have higher temperatures than night hours, the white area travels from left to right, then from right to left, starting from the daytime and ending with the nighttime. This visual understanding should aid in interpreting the data of the HFPs for the 12 parameters, which are shown in Fig. S. 35 to Fig. S. 42. Secondly, the following can be observed from Fig. S. 35 to Fig. S. 42 concerning the wind speed (parameter 1 of 12) profiles: (i) the HFPs of the hours from 00:00 to 05:00 and 18:00 to 23:00 reach upper-high wind speed ranges, and (ii) the HFPs of the hours from 06:00 to 17:00 stay within moderate wind speed ranges. Thirdly, after considering the results of the LOESS regression analyses for the wind resource (see Fig. 4) along with the HFPs (see Fig. S. 35 to Fig. S. 42), the following can be observed concerning the wind direction (parameter 2 of 12) profiles: (i) the HFPs of hours from 00:00 to 23:00 have a high concentrated range

wind direction close to 318 ° with high wind speeds, and (ii) the HFPs of hours from 00:00 to 23:00 have a low concentrated range wind direction close to 150 ° with high wind speeds. Fourthly, the following can be clearly observed from Fig. S. 35 to Fig. S. 42 concerning the atmospheric pressure (parameter 4 of 12) profiles, the frequency pattern of the atmospheric pressure is opposite to the ambient temperature (parameter 3 of 12). Finally, the following can be observed from Fig. S. 35 to Fig. S. 42 concerning parameters 5, 6, 7, 8, 9, 10, 11, and 12 of 12 (generation of the optimal 1, 2, 3, 4, 40, 46, 52, and 58-row configuration, respectively): (i) for the 00:00 to 01:00 (early-day) hours: the HFPs exceed the AFPs at the highest (full load) generation range and the majority of the moderate generation ranges, (ii) for the 03:00 to 06:00 (early-day) hours: the HFPs match the AFPs at the highest (full load) generation range and upper-moderate generation ranges, and (iii) for the 18:00 to 23:00 (late-night) hours: the HFPs exceed the AFPs at the highest (full load) generation range and upper-moderate generation ranges.

3.8. Full load generation at rated wind speed

This section evaluates the full load generation at the rated wind speed according to the wind turbine specifications (see Fig. 2 and Table 1) for the selected 8 of the 60 optimal configurations (i.e., for categories 1, 2, 3, 4, 40, 46, 52, and 58 of 60). Figs. 11 and 12 show that the optimal 1-row configuration (category 1 of 60) has the highest full load generation at the rated wind speed due to having the slightest wind disturbance and wake losses as it corresponds to a 1-row configuration (single row). It can be observed that the full load generation at the rated wind speed decreases as the N_r value increases. Furthermore, it can be observed that the full load generation at the rated wind speed is independent of θ_{plant}. It is concluded that the order from highest to lowest full load generation at the rated wind speed is as follows: the optimal 1, 2, 3, 4, 40, 46, 52, and 58-row configuration, respectively.

3.9. Economic analysis

This section performs an economic assessment for the 60 optimal configurations of the wind power plants based on the LCOE-minimization criterion. The impact of varying N_r and θ_{plant} on the financial indicators for these configurations is assessed. The following indicators are evaluated for the selected 8 of the 60 optimal configurations (i.e., several designs of mega-scale wind power plants): (i) the installed cost per watt, (ii) the present value of annual energy, (iii) the net present value (annual costs) with relation to annual energy and annual gross energy, (iv) the internal rate of return at the end of the analysis period, (v) the project return (after-tax project maximum internal rate of return), (vi) the required Power Purchase Agreement (PPA) price, (vii) the flip actual percentage, (vii) the flip target percentage, (ix) the flip target year, and (x) the cash flow over the project lifetime. Fig. 13 shows the installed cost per watt as a function of N_r for the 60 optimal configurations. For the selected 8 of the 60 optimal configurations, the corresponding installed costs are as follows: 2.0616, 2.0386, 2.0312, 2.0275, 2.0166, 2.0165, 2.0163, 2.0162 $/W, which correspond to the LCOE values of 5.76734, 5.94352, 6.0849, 6.15907, 6.08697, 6.0745, 6.06462, 6.05662 cent/kWh, respectively. From the analysis results, it can be concluded that there exists an exponential relation between the installed cost per watt and N_r.

Fig. S. 43 shows the present value of annual energy, the net present value (annual costs), the annual energy, and the annual gross energy as a function of N_r for the 60 optimal configurations. It is clear that these have increasing linear trends as N_r increases. Thus, there exist linear relations between these and N_r. Fig. S. 44 shows the internal rate of return at the end of the analysis period (25 years), the project return (i.e., after-tax project maximum internal rate of return), and the required PPA price. Fig. S. 45 shows multiple profiles for the 60 optimal design configurations of the wind power plants: the flip actual percentage, the flip target percentage, and the flip target year. Fig. S. 46 to Fig. S. 48

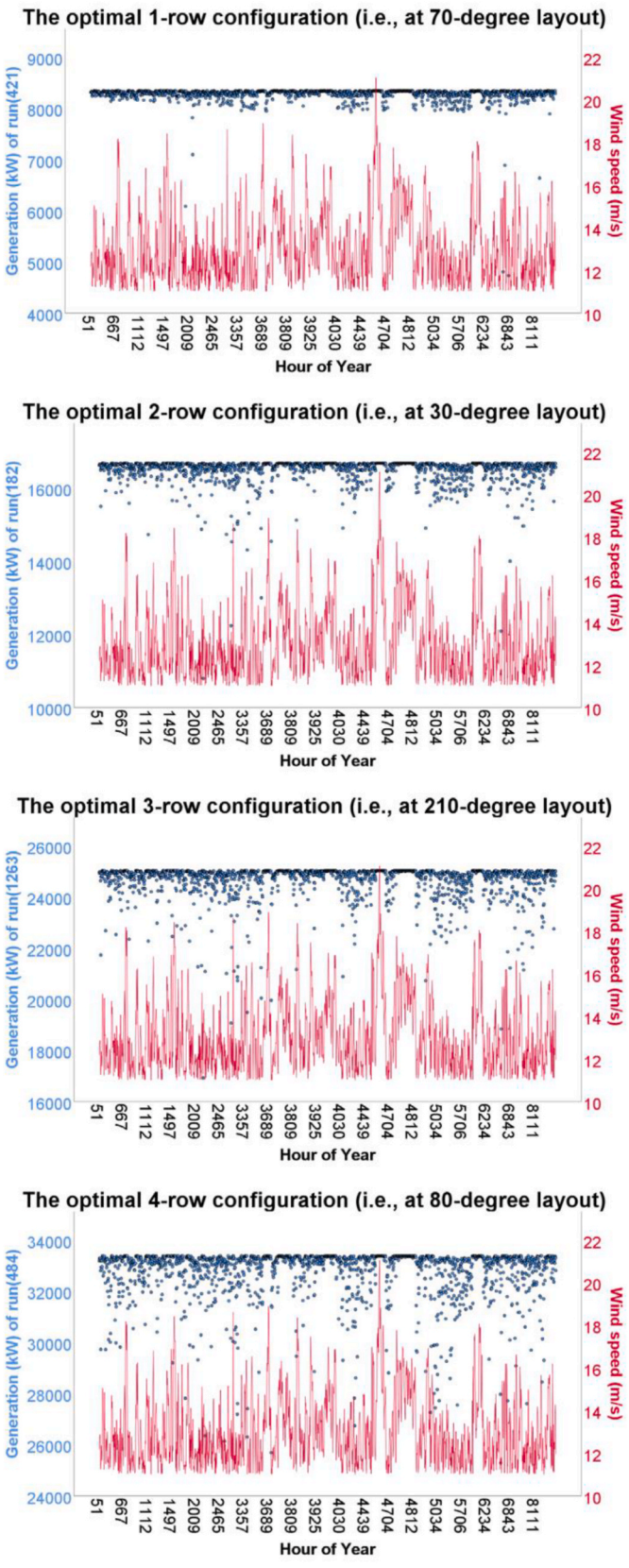

Fig. 11. Full load generation at the rated wind speed for selected 4 of the 60 optimal configurations (the optimal 1, 2, 3, and 4-row configurations) – (optimal low row-count configurations).

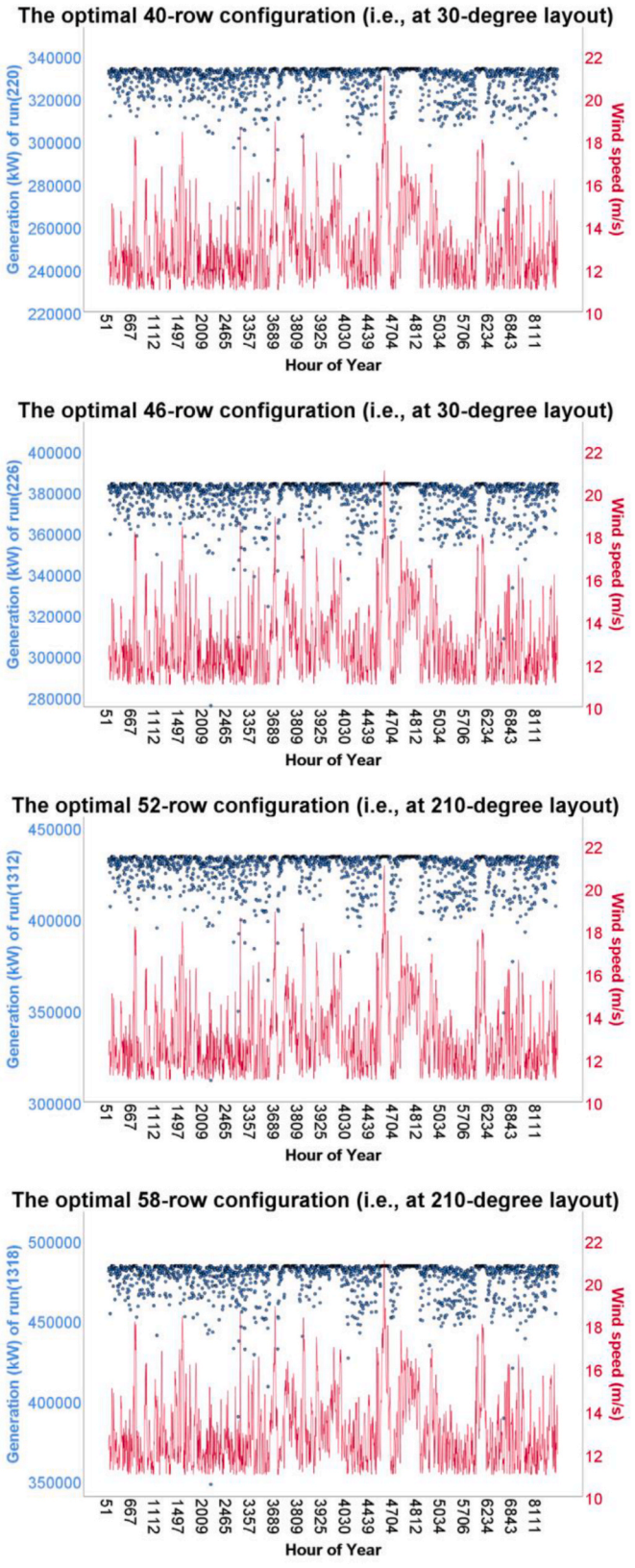

Fig. 12. Full load generation at the rated wind speed for selected 4 of the 60 optimal configurations (the optimal 40, 46, 52, and 58-row configurations) – (optimal high row-count configurations).

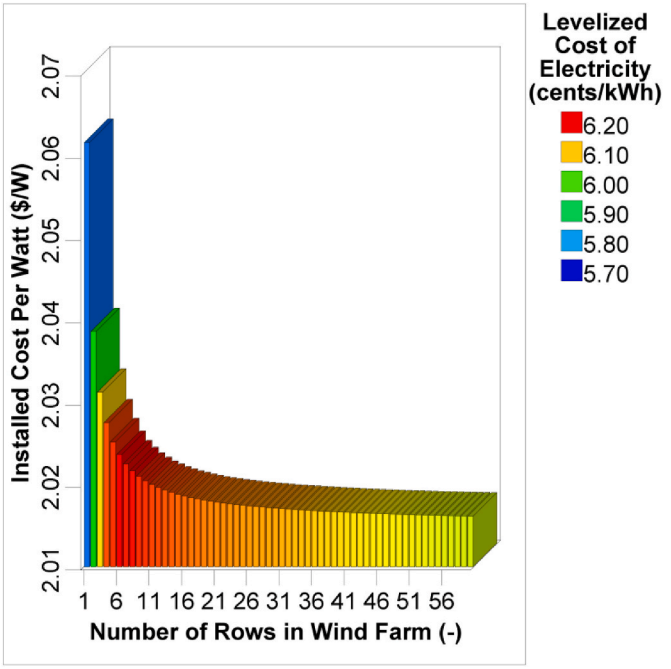

Fig. 13. The installed cost per watt as a function of N_r for the 60 optimal configurations of wind power plants (the optimal 1-row to 60-row configurations from left to right).

show the cash flow over the project lifetime (25 years) for the selected 8 of the 60 optimal configurations (i.e., for categories 1, 2, 3, 4, 40, 46, 52, and 58 of 60). The optimal configurations demonstrated profitability during the lifetime of these projects except for the initial year due to the CAPEX. It is revealed that the optimal configurations require a PPA price of at least 7.03 cent/kWh to make a positive return on investment.

4. Conclusion

In this work, one of the objectives is to assess the performance of multi-row design configurations for wind power plants. The configurations have optimal values of θ_{plant} that result in the lowest LCOE after an evaluation of 2220 different configurations. The optimal configurations are identified for various N_r values. The wind power potential is assessed both technically and economically. The study concludes that the values of N_r and θ_{plant} values impact factors, such as LCOE, wake losses, performance ratio, capacity factor, and annual gross energy.

Some of the findings are summarized as follows: (i) the α value is calculated to be 0.15 and more significant than 0.29 for the daytime and nighttime, respectively, The P_d value is calculated to be 289 W/ m^2 for a mean wind speed of 8.02 m/s, (ii) June and July have high levels of generation, wind speed, temperature, and humidity. Also, the wind speed is at maximal levels during the nighttime, leading to an increase in economic feasibility and reduction of curtailment from renewable power cogeneration if wind power is accompanied by solar technologies, such as CSP-PT/TES, after evaluating the wind and solar resources, (iii) the LOESS regression analyses confirmed that the wind direction and distribution ranges have consistent and robust northwest components throughout the year, (iv) 60 design configurations with optimal θ_{plant} values based on the LCOE-minimization criterion are identified with a linear increase in annual gross energy occurs as the N_r value increases for almost all ranges of θ_{plant}, (v) as the N_r value increases, an increase in the LCOE occurs for the following ranges of θ_{plant}: 110-140 ° and 280-320 ° (red areas). At small values of N_r, a decrease in the LCOE occurs for the following ranges of θ_{plant}: 0-75 °, 160-260 °, and 340-360 ° (dark-blue areas), (vi) as the N_r value increases, an increase in the wake losses

occurs for the following ranges of θ_{plant}: 110-140 ° and 280-320 ° (red areas). At small values of N_r, a decrease in the wake losses occurs for the following ranges of θ_{plant}: 0-75 °, 160-260 °, and 340-360 ° (dark-blue areas), (vii) as the N_r value increases, a decrease in the performance ratio occurs for the following ranges of θ_{plant}: 110-140 ° and 280-320 ° (dark-blue areas). At small values of N_r, an increase in the performance ratio occurs for the following ranges of θ_{plant}: 0-75 °, 160-260 °, and 340-360 ° (red areas), (vii) as the N_r value increases, a decrease in the capacity factor occurs for the following ranges of θ_{plant}: 110-140 ° and 280-320 ° (dark-blue areas). At small values of N_r, an increase in the capacity factor occurs for the following ranges of θ_{plant}: 0-75 °, 160-260 °, and 340-360 ° (red areas), (ix) the wind speed and direction frequencies have various impacts on the LCOE, wake losses, performance ratio, capacity factor, and annual gross energy once linked with the variation of N_r and θ_{plant}. Since there are more wind turbines for higher N_r values, the turbines create more turbulence at high wind speeds, leading to increased wake losses. As a result, the LCOE increases while the performance ratio, capacity factor, and generation decrease accordingly, (x) the monthly and hourly performance have been evaluated for the selected 8 of the 60 optimal configurations (i.e., for categories 1, 2, 3, 4, 40, 46, 52, and 58 of 60). It should be recognized that the optimal selection is based on the LCOE-minimization criterion, and the evaluations are performed considering the frequency profiles of 12 assessment parameters, (xi) it can be observed that the full load generation at the rated wind speed decreases as the N_r value increases. Furthermore, it can be observed that the full load generation at the rated wind speed is independent of θ_{plant}. Thus, the highest to lowest full load generation order at the rated wind speed is as follows: the optimal 1, 2, 3, 4, 40, 46, 52, and 58-row configuration, respectively.

For the selected 8 of the 60 optimal configurations (i.e., for categories 1, 2, 3, 4, 40, 46, 52, and 58 of 60), the corresponding installed costs are as follows: 2.0616, 2.0386, 2.0312, 2.0275, 2.0166, 2.0165, 2.0163, 2.0162 $/W, which correspond to the LCOE values of 5.76734, 5.94352, 6.0849, 6.15907, 6.08697, 6.0745, 6.06462, 6.05662 cent/kWh, respectively. Thus, it can be concluded that there exists an exponential relation between the installed cost per watt and N_r. Additionally, the present value of annual energy, net present value (annual costs), annual energy, and annual gross energy have increasing linear trends as N_r increases. Thus, there exist linear relations between these and N_r. Finally, it is revealed that the optimal configurations require a PPA price of at least 7.03 cent/kWh to make a positive return on investment.

CRediT authorship contribution statement

Ali J. Sultan: Conceptualization, Methodology, Software, Validation, Formal analysis, Investigation, Data curation, Visualization, Writing – original draft, Writing – review & editing. **Derek B. Ingham:** Writing – review & editing. **Lin Ma:** Writing – review & editing. **Kevin J. Hughes:** Writing – review & editing. **Mohamed Pourkashanian:** Writing – review & editing.

Declaration of competing interest

The authors declare that they have no known competing financial interests or personal relationships that could have appeared to influence the work reported in this paper.

Data availability

Data in the form of model input data is available in the appendices in the supplementary data.

Acknowledgments

This study was supported by the Kuwait Institute for Scientific Research. Thanks to the Kuwait Ministry of Electricity, Water, and Renewable Energy for making its fossil-based plant data available. For the purpose of open access, the author has applied a Creative Commons Attribution (CC BY) license to any author accepted manuscript version arising. Data in the form of model input data is available in the Appendices (Supplementary data) along with this work.

Appendix A. Supplementary data

Supplementary data to this article can be found online at https://doi.org/10.1016/j.jclepro.2023.139578.

References

Aeolos, 2020. Which factors will affect the annual energy output of the wind turbine? Hieff wind energy, ltd (Europe & America) [Available Online]. https://www.windturbinestar.com/wind-turbine-annual-output.html.

Al-Dousari, A., Ibrahim, M., Al-Dousari, N., Ahmed, M., Al-Awadhi, S., 2018. Pollen in aeolian dust with relation to allergy and asthma in Kuwait. Aerobiologia 34 (3), 325–336. https://doi.org/10.1007/s10453-018-9516-8.

Al-Dousari, A W Al-Nassar, Al-Hemoud, A., Alsaleh, A., Ramadan, A., Al-Dousari, N., Ahmed, M., 2019. Solar and wind energy: challenges and solutions in desert regions. Energy 176, 184–194. https://doi.org/10.1016/j.energy.2019.03.180.

Al-Dousari, Ali, Waleed, Al-Nassar, Ahmed, Modi, 2020. Photovoltaic and wind energy: challenges and solutions in desert regions. In: E3S Web of Conferences, vol. 166. EDP Sciences. https://doi.org/10.1051/e3sconf/202016604003.

Al-Nassar, W.K., Neelamani, S., Al-Salem, K.A., Al-Dashti, H.A., 2019. Feasibility of offshore wind energy as an alternative source for the state of Kuwait. Energy 169 (February), 783–796. https://doi.org/10.1016/j.energy.2018.11.140.

Al-Rasheedi, Majed, Chris Gueymard, Al-Hajraf, Salem, Ismail, Alaa, 2015. Solar resource assessment over Kuwait: validation of satellite-derived data and reanalysis modeling. In: EuroSun 2014, Aix-Les-Bains. https://doi.org/10.18086/eurosun.2014.08.01 *(France), 16 – 19 September 2014*, 1–10.

Al-Salem, Khaled, Al-Nassar, Waleed, 2018. Assessment of wind energy potential at Kuwaiti islands by statistical analysis of wind speed data. In: E3S Web of Conferences, vol. 51. EDP Sciences. https://doi.org/10.1051/e3sconf/20185101001.

Alhajraf, S., Heil, O., 2011. Feasibility Study of Renewable Energy Technologies in the State of Kuwait. Project No. EU060C. Report No. KISR 10673. Kuwait Institute for Scientific Research (KISR). Final Report. https://epa.org.kw/Portals/0/PDF/advancement-science8.pdf.

Alhajraf, S., Alabdullah, Y., Sultan, A.J., Alnahedh, S., Alnassar, W., Alsenafy, M., Alibrahim, I., Alawadhi, A., Ameer, B., 2011. Performance Assessment of Renewable Energy Applications in the State of Kuwait. Final Report. EU057C. Kuwait Institute for Scientific Research (KISR), 2011.

Ali, Hussain, Alsabbagh, Maha, 2018. Residential electricity consumption in the state of Kuwait. Environment Pollution and Climate Change 2 (1). https://doi.org/10.4172/2573-458x.1000153.

Alnassar, W., Alhajraf, S., Alenizi, A., Alawadhi, L., 2005. Potential wind power generation in the state of Kuwait. November 2005 Renew. Energy 30 (14), 2149–2161. Https://Doi.Org/10.1016/j.Renene.2005.01.002." 2005. https://wwwsciencedirectcom/science/article/pii/S0960148105000145#fig5.

Alrai, 2015. Newspaper Article in Arabic [Online]. Alrai Media Group (Newspaper). Published: 29 September 2015.," 2015. http://www.alraimedia.com/Home/Details?id=53ab9db2-2245-4fd7-8d91-c5caf47a1d57.

Alrashidi, M.S., Alsudairawi, M., Ramadan, A., An, Aldabbous, Sultan, A.J., 2011. Air Quality Assessment in the Ali Sabah Alsalem Urban Community, Phase II. KISR 10656. Kuwait Institute for Scientific Research (KISR), 2011.

Ansari, M., 2013. Kuwait Utilities Sector. Industry Research. http://www.infomercatiesteri.it/public/images/paesi/107/files/Kuwait Utilities Sector Report_pdf 6_13.pdf.

Ashurst, 2016. Renewables in Morocco [Online]. Africa Energy Forum, 2016. https://www.ashurst.com/en/news-and-insights/legal-updates/renewables-in-morocco—june-2016/.

Atalla, Tarek N., Hunt, Lester C., 2016. Modelling residential electricity demand in the GCC countries. Energy Econ. 59 (September), 149–158. https://doi.org/10.1016/j.eneco.2016.07.027.

Branker, K., Pathak, M.J.M., Pearce, J.M., 2011. A review of solar photovoltaic levelized cost of electricity. Renew. Sustain. Energy Rev. 15 (9), 4470–4482. https://doi.org/10.1016/j.rser.2011.07.104.

Burt, Christopher C., 2016a. Chris Burt: hottest reliably measured air temperatures on earth, 2016. http://www.markvoganweather.com/2016/07/29/chris-burt-hottest-reliably-measured-air-temperatures-on-earth/.

Burt, Christopher C., 2016b. Hottest reliably measured air temperatures on earth, 2016. https://www.wunderground.com/blog/weatherhistorian/hottest-reliably-measured-air-temperatures-on-earth.html.

Fares, Mohamed Soufiane Ben, Abderafi, Souad, 2018. Water consumption analysis of Moroccan concentrating solar power station. Sol. Energy 172 (September), 146–151. https://doi.org/10.1016/j.solener.2018.06.003.

Fletcher, Steven, 2016. 'The World's Hottest Day EVER Is Recorded in Kuwait as Temperature Soars to 54C' [Online]. Daily Mail, Mail Online, News. Published by Associated Newspapers Ltd, Part of the Daily Mail. The Mail on Sunday & Metro Media Group, 2016. https://www.dailymail.co.uk/news/article-3704601/The-hottest-day-recorded-Kuwait-temperature-soars-54C.html.

GENI, 2017. National Energy Grid Kuwait. Global Energy Network Institute. 4420 Rainier Avenue, Suite 308, San Diego, California 92120 USA, 2017. http://www.geni.org/globalenergy/library/national_energy_grid/kuwait/kuwaitnationalelectricitygrid.shtml.

Hamilton, William T., Alexandra, M. Newman, Wagner, Michael J., Braun, Robert J., 2020. Off-design performance of molten salt-driven rankine cycles and its impact on the optimal dispatch of concentrating solar power systems. Energy Convers. Manag. 220 (September) https://doi.org/10.1016/j.enconman.2020.113025.

Hertog, Steffen, 2013. The private sector and reform in the Gulf cooperation Council countries. In: Kuwait Programme on Development; Governance and Globalisation in the Gulf States. No. 30. London School of Economics and Political Science, 2013. http://eprints.lse.ac.uk/54398/1/Hertog_2013.pdf.

Ho, C.K., 2008. SANDIA. Software and Codes for Analysis of Concentrating Solar Power Technologies. Sandia National Laboratories, 2008. https://www.Osti.Gov/Biblio/946571.

Hoffmann, W., 2010. PV Solar Electricity in EUMENA: Headway in the World. Mediterranean Solar Plan-Introduction. European Photovoltaic Industry Association (EPIA), Valencia. May 11th 2010. https://www.dissercat.com/content/issledovanie-effektivnosti-skhem-energosnabzheniya-avtonomnykh-potrebitelei-v-afrike-na-osno.

IRENA, 2012. Renewable energy technologies: cost analysis series concentrating solar power volume 1: power sector issue 2/5 acknowledgement. www.irena.org/Publications.

IRENA, 2014. Renewables readiness assessment: sultanate of Oman. A report by the international renewable energy agency. http://www.irena.org/publications/2014/Nov/Renewables-Readiness-Assessment-Sultanate-of-Oman.

IRENA, 2016. Renewable Energy Market Analysis: the GCC Region. A Report by the International Renewable Energy Agency. https://doi.org/10.1017/S1740355311000283.

IRENA, 2018. Renewable Power Generation Costs in 2017, A Report by the International Renewable Energy Agency. International Renewable Energy Agency, Abu Dhabi, UAE. https://doi.org/10.1007/SpringerReference_7300, 2018.

ISES, 2018. Concentrating solar thermal power with built in storage. A webinar by the international solar energy society (ISES). Jan 2018." 2018. https://www.youtube.com/watch?v=9oxR7BNx8nU.

Khatti, Shakir Shakoor, Woodruff, George W., 2021. Techno-Economic Optimization and Market Potential Study of Small-Scale Particle Heating Receiver Based Central Receiver Power Tower Plants in Mena Region. A Dissertation Presented to The Academic Faculty." Georgia Institute of Technology. https://smartech.gatech.edu/handle/1853/64679.

Livingston, Ian, 2019. 'Scorching temperatures in Kuwait and Pakistan among hottest measured' [online], 2019. https://www.smh.com.au/environment/climate-change/scorching-temperatures-in-kuwait-and-pakistan-among-hottest-measured-20190619-p51z4k.

Mirza, Adal, 2018. 'Kuwait looks at crude oil expansion as neutral zone row drags' [online], 2018. https://www.platts.ru/news-feature/2018/oil/2018-oil-natgas-outlook/2018-kuwait-crude-expansion.

Mohideen, Mohamedazeem M., Balachandran, Subramanian, Jingyi, Sun, Jing, Ge, Han, Guo, Adiyodi Veettil, Radhamani, Seeram, Ramakrishna, Yong, Liu, 2023. Techno-economic analysis of different shades of renewable and non-renewable energy-based hydrogen for fuel cell electric vehicles. Renew. Sustain. Energy Rev. 174 (March), 113153 https://doi.org/10.1016/J.RSER.2023.113153.

MOO, 2016. Kuwait Oil Field Map. Kuwait Ministry of Oil, 2016. http://www.moo.gov.kw/About-Us/Programs/Technical-Affairs/Kuwait-Oil-Field-Map.aspx.

NREL, 2019. System Advisor Model (SAM). National Renewable Energy Laboratory. https://sam.nrel.gov/download.html.

Ritchie, Hannah, Roser, Max, 2014. Energy. Our world in data, 2014. [Online]." 2014. https://ourworldindata.org/energy.

Ritchie, Hannah, Roser, Max, 2017. CO_2 and Greenhouse Gas Emissions. Our World in Data, 2017. [Online]." 2017. https://ourworldindata.org/co2-and-other- greenhouse-gas-emissions.

Sebzali, M., Sultan, A.J., Altabtabaei, M., 2016. Design of Self-Reliant, Sustainable Protected Environment Food Protection System. Int. Report. EA070K. Kuwait Institute for Scientific Research (KISR), 2016.

Shams, H.M., Bradley, D.A., Regan, P.H., 2017. Determination of levels of naturally occurring radioactive materials in lagoon samples containing produced water from the minagish oil field in the state of Kuwait. Radiat. Phys. Chem. 137 (August), 193–197. https://doi.org/10.1016/j.radphyschem.2016.03.006.

Short, Walter, Packey, Daniel J., Holt, Thomas, 1995. A Manual for the Economic Evaluation of Energy Efficiency and Renewable Energy Technologies.

SolarGIS, 2019. Solar Resource Maps of Kuwait, 2019. https://solargis.com/maps-and-gis-data/download/kuwait.

Sultan, A.J., 2017. An Exergy-Based Approach for Performance Assessment of a Solar Thermal Energy Collecting Converting System. Final Report. EA048G. Kuwait Institute for Scientific Research (KISR), 2017.

Sultan, A.J., Alotaibi, A., 2016. Feasibility of Implementing Photovoltaic Systems at Kuwait National Petroleum Company Premises. EA005S. KISR 13336. Kuwait Institute for Scientific Research (KISR).

Sultan, AJ, Hughes, KJ, Ingham, DB, Ma, L, Pourkashanian, M, 2020a. Supplementary Material for Research Article 110342 "Techno-Economic Competitiveness of 50 MW Concentrating Solar Power Plants for Electricity Generation under Kuwait Climatic Conditions". Renewable and Sustainable Energy Reviews 134, 110342. https://doi.org/10.1016/j.rser.2020.110342 (download from "Appendix A. Supplementary data" in DOI).

Sultan, AJ, Hughes, KJ, Ingham, DB, Ma, L, Pourkashanian, M, 2020b. Techno-Economic Competitiveness of 50 MW Concentrating Solar Power Plants for Electricity Generation under Kuwait Climatic Conditions. Renewable and Sustainable Energy Reviews 134, 110342. https://doi.org/10.1016/j.rser.2020.110342.

Sultan, AJ, Ingham, DB, Hughes, KJ, Ma, L, Pourkashanian, M, 2021a. Supplementary Material for Research Article 111411 "Optimization and Performance Enhancement of Concentrating Solar Power in a Hot and Arid Desert Environment". Ren. Sustain. Energy Rev. 149 (2021), 111411. https://doi.org/10.1016/j.rser.2021.111411 (download from "Appendix A. Supplementary data" in DOI). https://doi.org/10.1016/J.RSER.2021.111411.

Sultan, AJ, Ingham, DB, Hughes, KJ, Ma, L, Pourkashanian, M, 2021b. Optimization and Performance Enhancement of Concentrating Solar Power in a Hot and Arid Desert Environment. Renew. Sustain. Energy Rev. 149 (2021), 111411. https://doi.org/10.1016/J.RSER.2021.111411.

Trabelsi, Seif Eddine, Chargui, Ridha, Qoaider, Louy, Ahmed, Liqreina, Amen, Allah Guizani, 2016. Techno-economic performance of concentrating solar power plants under the climatic conditions of the southern region of Tunisia. Energy Convers. Manag. 119, 203–214. https://doi.org/10.1016/j.enconman.2016.04.033.

Wagner, M., 2008. Simulation and predictive performance modeling of utility-scale central receiver system power plants. https://www.researchgate.net/publication/44205074.

Wagner, M., Gilman, P., 2011. Technical manual for the SAM physical trough model. A Report by NREL. https://www.nrel.gov/docs/fy11osti/51825.pdf.

WMO, 2019. 'WMO verifies 3rd and 4th hottest temperature recorded on earth' [online], 2019 An Article by the World Meteorological Organization. https://public.wmo.int/en/media/press-release/wmo-verifies-3rd-and-4th-hottest-temperature-recorded-earth.

World Bank, 2019b. World development indicators (2019). GDP per capita. World Bank. [Online]." 2019 https://data.worldbank.org/indicator/NY.GDP.PCAP.CD.